

# Nonlinear Analysis of Shells Using the MITC Formulation<sup>†</sup>

Eduardo N. Dvorkin

Center for Industrial Research, FUDETEC  
Av. Córdoba 320  
1054, Buenos Aires, Argentina

## Summary

The formulation of general shell elements using the method of mixed interpolation of tensorial components (MITC) is reviewed. In particular three elements that were formulated using the MITC method are examined: the MITC4 and MITC8 that were developed for general nonlinear analysis under the restriction of small strains and the MITC4-TLH that was developed for finite strain elasto-plastic analysis of shells.

## 1. INTRODUCTION

In 1970 Ahmad, Irons and Zienkiewicz [1,2] established the bases on which, most of the work that has been done since then on finite element analysis of shell structures, was built: they published the *isoparametric shell element* with independent  $C^0$  interpolations for displacements and rotations. From now on we will refer to this element as the A-I-Z shell element.

The most relevant aspect of the A-I-Z shell element is that the interpolation functions require only  $C^0$  continuity. However the price for this low order continuity requirement is the introduction of shear deformations in the formulation. These elements are therefore generically known as Reissner / Mindlin shell elements [3,4].

The A-I-Z shell element was very naturally developed from the 3D continuum isoparametric element formulation via the imposition of kinematic constraints [2].

Even though the introduction of shear deformations in the formulation seems to be desirable for the analysis of thick shells, and also makes very natural the transition from 3D to shell elements [5,6], these shear deformations cause the main numerical difficulty of the A-I-Z element: the *locking* phenomenon [2,6].

The extension of the A-I-Z shell element for nonlinear analysis (small strains) was independently developed by Ramm [7] and by Kråkeland [8].

In Section 2 we will review the A-I-Z shell element formulation, its locking problem and the first remedies that were proposed to relieve it: reduced / selective numerical integration schemes. In that Section we will also review the drawbacks of those remedies.

Most of the research developed in the area of finite element analysis of shells since 1970 has been devoted to elements that while being based on the A-I-Z element try to overcome the locking problem.

In this paper we will concentrate on the *method of mixed interpolation of tensorial components* (MITC) introduced by Bathe and Dvorkin [9-13].

In Section 3 we will review the linear formulations of the MITC4 and MITC8 shell elements, while in Section 4 we will comment on the material and geometric nonlinear formulation restricted to small strains of the above elements. In Section 5 we will review the formulation that we recently developed for finite strain elasto-plastic analysis of shells using the MITC4 shell element.

---

<sup>†</sup> In memoriam of Juan Carlos Simo

## 2. THE AHMAD-IRONS-ZIENKIEWICZ SHELL ELEMENT

A typical A-I-Z shell element is depicted in Figure 1. In order to define its configuration at a given time (load level)  $t$  we use [6]:

- The coordinates of the mid-surface nodes referred to a global Cartesian system  $\{^t x_i, i = 1, 2, 3\}$ , with base vectors  $^t \underline{e}_i$ .
- Director vectors defined at the mid-surface nodes. These nodal director vectors are defined so as to approximate as closely as possible the shell normal at those nodes.

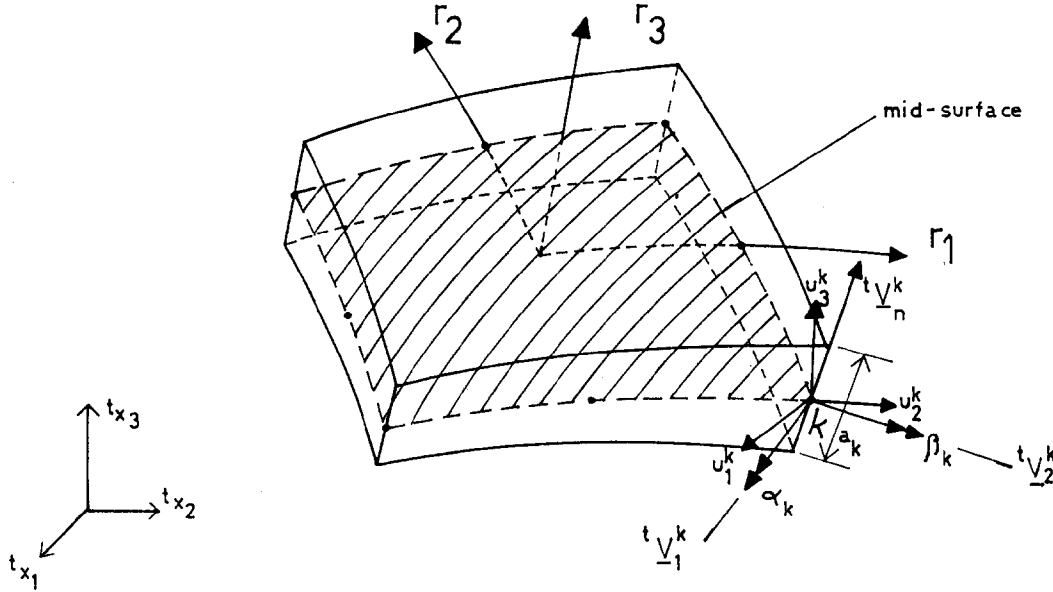


Figure 1. Ahmad-Irons-Zienkiewicz shell element

An arbitrary point inside the shell element is defined by its natural coordinates  $\{r_i, i = 1, 2, 3\}$  and the position vector of that point is given by the following interpolation [6]

$$^t \underline{\mathbf{x}} = h_k(r_1, r_2) ^t \underline{\mathbf{x}}_k + \frac{r_3}{2} h_k(r_1, r_2) ^t a_k ^t \underline{\mathbf{V}}_n^k \quad (1)$$

( $t = 0$  represents the underformed configuration used as *reference configuration* in what follows).

In Eqn. (1) we use the summation convention, and:

$h_k(r_1, r_2)$ : 2D isoparametric interpolation functions corresponding to the  $k$ -th mid-surface node [2,6].

$^t \underline{\mathbf{x}}_k$ : position vector of the  $k$ -th mid-surface node at time  $t$ .

$^t a_k$ : shell thickness at the  $k$ -th mid-surface node at time  $t$ .

$^t \underline{\mathbf{V}}_n^k$ : director vector corresponding to the  $k$ -th mid-surface node at time  $t$ , defined taking into account that  $|^t \underline{\mathbf{V}}_n^k| = 1$ .

It is evident that by using the interpolation defined by Eqn. (1) we can model shells of variable thickness.

Using Eqn. (1) we can interpolate the geometry of any 3D solid. For the case of shells the following additional *kinematic constraints* are introduced [1,2,6]:

- The director vectors remain straight during the deformation process.
- The thickness remains constant during the deformation process ( ${}^{t+\Delta t}a_k = {}^t a_k = \dots = {}^\circ a_k$ ).

It is evident that the second constraint is only suitable to describe the kinematics of infinitesimal strain deformation processes (see Section 5).

Considering a linear kinematic description (infinitesimal displacements, rotations and strains), the rotations can be considered as vectors and, for the incremental displacements from the configuration at  $t$  to a configuration at  $t + \Delta t$  we get

$$\underline{\mathbf{u}} = {}^{t+\Delta t}\underline{\mathbf{x}} - {}^t\underline{\mathbf{x}} = h_k \underline{\mathbf{u}}_k + \frac{r_3}{2} h_k {}^t a_k (-\alpha_k {}^t\underline{\mathbf{V}}_2^k + \beta_k {}^t\underline{\mathbf{V}}_1^k) \quad (2)$$

In the above equation:

$\underline{\mathbf{u}}_k$ : incremental displacement of the k-th mid-surface node.

$\alpha_k, \beta_k$ : incremental rotations at the k-th mid-surface node around the vectors  ${}^t\underline{\mathbf{V}}_1^k$  and  ${}^t\underline{\mathbf{V}}_2^k$ .

The auxiliary vectors  ${}^t\underline{\mathbf{V}}_1^k$  and  ${}^t\underline{\mathbf{V}}_2^k$  are depicted in Figure 1 and are defined as

- If  ${}^t\underline{\mathbf{e}}_2 \times {}^t\underline{\mathbf{V}}_n^k \neq \underline{\mathbf{0}}$

$${}^t\underline{\mathbf{V}}_1^k = \frac{{}^t\underline{\mathbf{e}}_2 \times {}^t\underline{\mathbf{V}}_n^k}{|{}^t\underline{\mathbf{e}}_2 \times {}^t\underline{\mathbf{V}}_n^k|} \quad (3.a)$$

$${}^t\underline{\mathbf{V}}_2^k = {}^t\underline{\mathbf{V}}_n^k \times {}^t\underline{\mathbf{V}}_1^k \quad (3.b)$$

- If  ${}^t\underline{\mathbf{e}}_2 \times {}^t\underline{\mathbf{V}}_n^k = \underline{\mathbf{0}}$

$${}^t\underline{\mathbf{V}}_1^k = {}^t\underline{\mathbf{e}}_3 \quad (3.c)$$

$${}^t\underline{\mathbf{V}}_2^k = {}^t\underline{\mathbf{e}}_1 \quad (3.d)$$

Obviously, in a computational implementation we adopt the second definition if  $|{}^t\underline{\mathbf{e}}_2 \times {}^t\underline{\mathbf{V}}_n^k| < \text{TOLN}$  where TOLN is some small number.

Please notice that the kinematic description given in Eqn. (2) implies that the formulation considers only 5 d.o.f. / mid-surface node (no drilling d.o.f.).

## 2.1 The locking problem

In order to introduce the shear locking phenomenon we recourse to a very simple example.

Let us consider a two-node beam element (Fig. 2.a) formulated following the A-I-Z approach (a Timoshenko beam element because shear deformations are included in the formulation [6]). The transversal displacement and in-plane rotation interpolations are

$$u_2 = h_1 u_2^1 + h_2 u_2^2 \quad (4.a)$$

$$\theta = h_1 \theta^1 + h_2 \theta^2 \quad (4.b)$$

The above linear interpolation functions satisfy the  $C^0$  continuity requirement.

For a very thin shell, the Bernoulli condition has to be fulfilled by the displacements and rotations

$$\gamma = \frac{du_2}{dx_1} - \theta \equiv 0 \quad (5)$$

With the interpolations defined by Eqns. (4), the constraint in Eqn. (5) leads to

$$\theta = \text{const} \quad (6)$$

and therefore in order to satisfy the boundary conditions at node 1 ( $\theta = 0$  because the node is fixed) we must have  $\theta = 0$  all over the element: *locking* behavior.

This shear locking is due to the fact that the functions used to interpolate  $u_2$  and  $\theta$  cannot satisfy the condition of zero shear strain all over the element.

It is important to notice that the source of the locking problem is the fact that the interpolation functions are unable to represent a state of pure bending with zero shear stresses, regardless of the use of finite or exact algebra.

We used a simple two node beam element to present a picture of shear locking. More rigorously we can study a general plate element [6,14]. The potential energy functional is for a linear elastic plate element in the  $(x_1 - x_2)$  plane

$$\pi = \frac{h^3}{2} \left[ \int_A \underline{\kappa}^T \underline{\mathbf{C}}_b \underline{\kappa} dA + \xi \int_A \underline{\gamma}^T \underline{\mathbf{C}}_s \underline{\gamma} dA \right] - V \quad (7)$$

where for a plate lying in the  $(x_1 - x_2)$  plane

$$\underline{\kappa} = \begin{bmatrix} \frac{\partial \beta}{\partial x_1} \\ -\frac{\partial \alpha}{\partial x_2} \\ \frac{\partial \beta}{\partial x_2} - \frac{\partial \alpha}{\partial x_1} \end{bmatrix} ; \quad \underline{\gamma} = \frac{1}{L} \begin{bmatrix} \frac{\partial u_3}{\partial x_1} - \beta \\ \frac{\partial u_3}{\partial x_2} + \alpha \end{bmatrix}$$

$$\underline{\mathbf{C}}_b = \frac{E}{12(1-\nu^2)} \begin{bmatrix} 1 & \nu & 0 \\ \nu & 1 & 0 \\ 0 & 0 & \frac{(1-\nu)}{2} \end{bmatrix} ; \quad \underline{\mathbf{C}}_s = \frac{k E}{2(1+\nu)} \begin{bmatrix} 1 & 0 \\ 0 & 1 \end{bmatrix}$$

$h$ : plate thickness

$L$ : element length

$E$ : Young's modulus

$\nu$ : Poisson's ratio

$k$ : shear correction factor [6]

$$\xi = \left(\frac{L}{h}\right)^2 \xrightarrow{h \rightarrow 0} \infty$$

$V$ : potential of external loads [6].

In the above,

$${}^\circ \underline{\mathbf{V}}_1 = \underline{\mathbf{e}}_1 ; \quad {}^\circ \underline{\mathbf{V}}_2 = \underline{\mathbf{e}}_2 ; \quad {}^\circ \underline{\mathbf{V}}_n = \underline{\mathbf{e}}_3$$

As the plate gets thinner, we can interpret the second integral on the r.h.s. of Eqn. (7) as a penalty term that imposes the constraint  $\underline{\gamma} \equiv \underline{\mathbf{0}}$ .

Therefore if the interpolation functions cannot represent  $\underline{\gamma} \equiv \underline{\mathbf{0}}$  (Kirchhoff-Love hypothesis)  $\xi$  will amplify any error in  $\underline{\gamma}$  as the plate gets thinner, leading to a locking behavior.

In order to introduce the membrane / shear locking [15] we again use a very simple example. Let us consider the planar curved three-node Timoshenko beam element under constant bending shown in Figure 2.b.

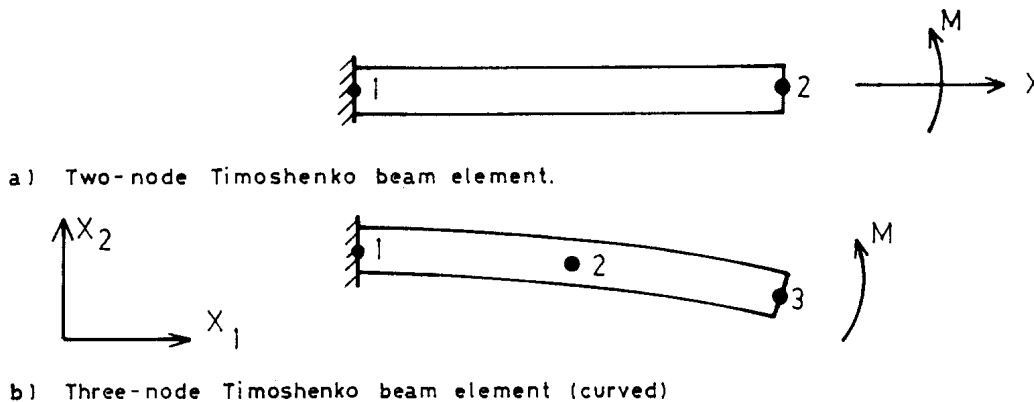


Figure 2. Simple problems illustrating the locking phenomenon

The functional of the potential energy is

$$\pi = \frac{E I}{2} \left[ \int_0^L \theta_{,s}^2 ds + \xi_M \int_0^L u_{s,s}^2 ds + \xi_S \int_0^L (u_{n,s} - \theta)^2 ds \right] - V \quad (8)$$

where  $L$  is the length of the curved beam measured along its axis, the  $s$ -direction is tangential to the beam axis and the  $n$ -direction is normal to the beam axis.

In the curved beam we use independent interpolations for  $u_1, u_2$  and  $\theta$ . As it is well known we cannot use independent interpolations for  $u_n, u_s$  and  $\theta$  because they would not contain the rigid body modes.

Since,  $\xi_M = \frac{12}{h^2}$  and  $\xi_S = \frac{6k}{(1+\nu)h^2}$  it is evident that in a pure bending situation when the beam gets thinner, the second and third integrals act as penalty terms to impose the conditions of zero stretching of the beam axis and zero shear strains

$$\epsilon_{ss} = u_{s,s} = 0 \quad (9.a)$$

$$\gamma_{ns} = u_{n,s} - \theta = 0 \quad (9.b)$$

If we prescribe  $\theta_i (i = 1, 2, 3)$  corresponding to the analytical solution of a constant bending problem, the boundary condition  $u_1^1 = u_2^1 = 0$  and try to calculate the remaining displacements by imposing Eqns. (9) at each of the three Gauss points we are left with a system of 6 equations with three unknowns which in general cannot be solved, demonstrating therefore the combined shear / membrane locking.

In Figure 3 we present some numerical results illustrating on this locking problem.

By a detailed inspection of the results in Figure 3 we can infer that locking is related to the element ratio ( $L \setminus h$ ) and not to the structural dimensions [14].

## 2.2 Reduced / selective integration as a remedy for the locking problem

The use of reduced / selective integration [16] was the first remedy that researchers found for the locking problem and for a long time it was the only resource that was available for engineering analyses of shell and plate structures.

However, the introduction of spurious zero energy modes [2,6] in the reduced and selective integrated element formulations lowers the reliability of their numerical results.

Many examples are reported in the literature illustrating the fact that reduced / selective integration is not a reliable procedure for engineering analyses. Among them:

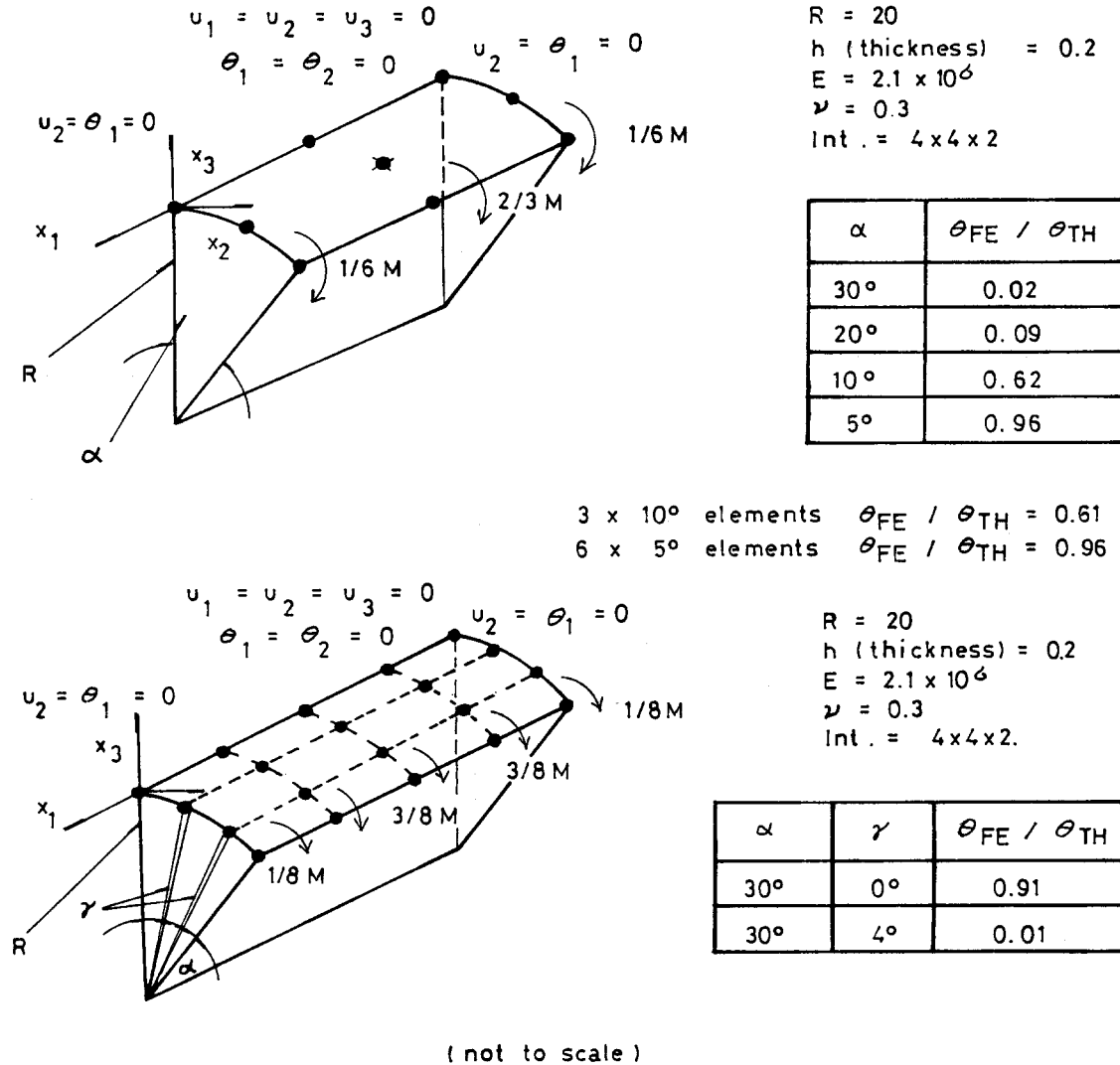


Figure 3. Numerical examples showing locking (A-I-Z elements)

- In Ref. [2, Chapter 11] Zienkiewicz and Taylor present some examples where the use of reduced integrated elements leads to erroneous results.
- Spurious oscillations in the transverse displacement results corresponding to a thick circular clamped plate modelled using selective integrated Lagrange elements are reported by Hughes in Ref. [17, Chapter 5].
- For nonlinear analysis in Refs. [9,13] we report a simple case that shows a spurious collapse behavior triggered by the spurious modes present in a reduced integrated element formulation.

It is important to point out that in the previous examples the elements assembly locked the spurious modes; and therefore the stiffness matrices (the initial stiffness matrix for the nonlinear case) were non-singular. Hence, the spurious modes present in an element

formulation can produce undesirable results even if they are restrained by the elements assembly.

It has been shown by Malkus and Hughes [18] that reduced and selective integration methods are equivalent to mixed formulations (for the simple case of a two-node Timoshenko beam element see also Refs. [9,19]). However, in reduced / selective integration methods once the integration rule is established the mixed formulation is obtained without any specific control over its performance. Hence drawbacks like the presence of spurious zero energy modes cannot be avoided except that reduced / selective integration schemes are used together with some stabilization procedures [20,21].

In the next Section we follow a different approach: a mixed formulation is custom-tailored to fulfil a criteria that we have established to assure *reliable results* in finite element analyses of shell structures (linear and nonlinear).

### 3. THE METHOD OF MIXED INTERPOLATION OF TENSORIAL COMPONENTS

To formulate a shell element using the MITC method we have to go through the following steps:

- (i) Select displacement / rotation interpolations.
- (ii) Select strain interpolations.
- (iii) Tie both interpolations together at selected sampling points.

By making a proper selection in each of the above items the *element designer* is able to custom-tailor the element formulation in order to fulfil her/his expectations on the new element performance.

By following the above procedure we obtain a non-conforming element, hence Irons' Patch Test [2,22] is the mandatory tool to *legalize* the formulation.

#### 3.1 The MITC4 shell element

The four-node MITC4 shell element formulation was designed so as to fulfil the following reliability criteria [9-13,23]:

- The element should not lock and should not contain spurious rigid body modes.
- The element should satisfy Irons' Patch test.
- It should be possible to use the element in non-flat geometries (it should be a shell element rather than a plate element).
- The element should be formulated for general nonlinear analysis. The original formulation [9-11] was developed, like most of the existing shell elements, under the constraint of small strains. The extension to finite deformations was presented in Ref. [23].
- It should be possible to use the element for the modelling of thin and moderately thick plates (where the condition of zero stresses through the thickness is still acceptable).

In Figure 4 we present the element description. In that figure  $\underline{\mathbf{g}}_i (i = 1, 2, 3)$  are the covariant base vectors of the element natural coordinate system.

The geometrical description and kinematics of the element (displacement / rotation interpolations) are the ones corresponding to the four-node standard A-I-Z shell element (see Eqns. (1) to (3)).

In the natural coordinate system of the element the strain tensor is written as

$$\underline{\underline{\boldsymbol{\epsilon}}} = \tilde{\epsilon}_{ij} \underline{\mathbf{g}}^i \underline{\mathbf{g}}^j \quad (10)$$

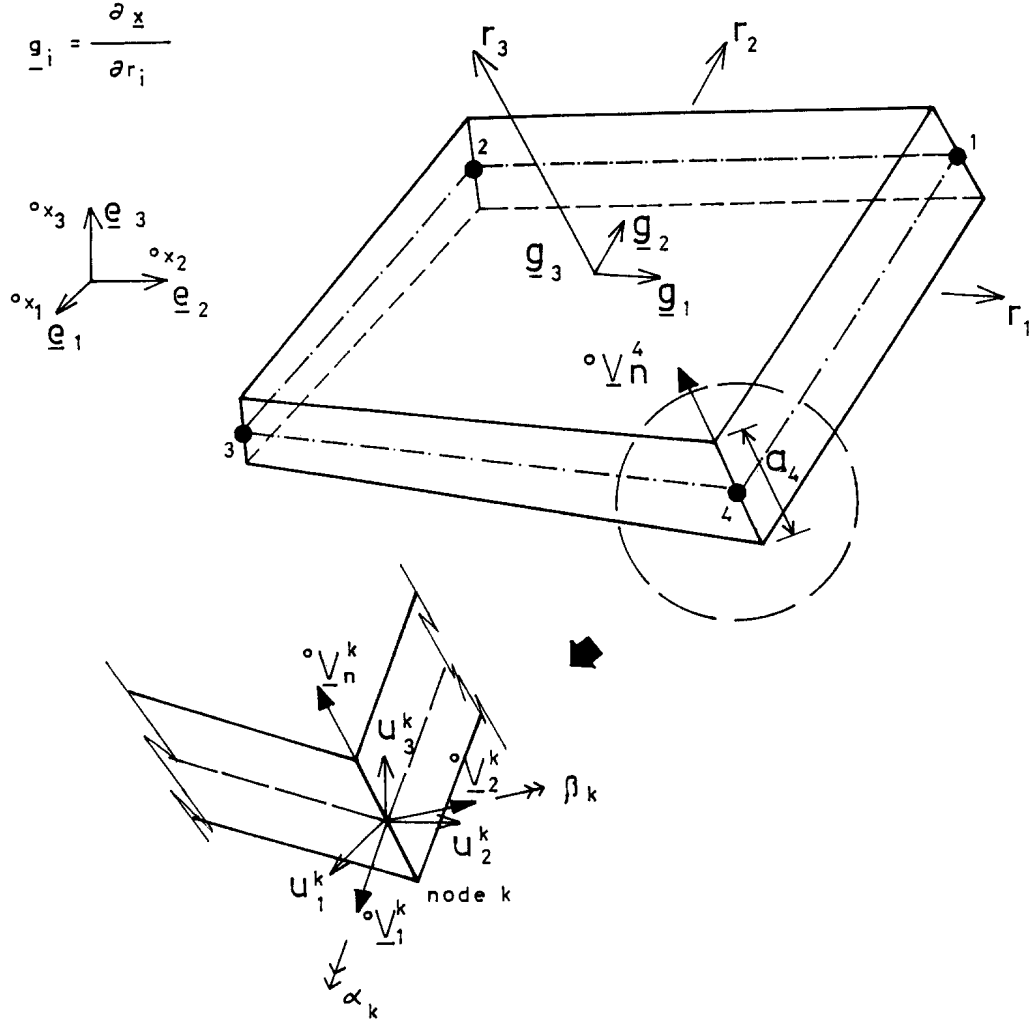


Figure 4. MITC4 shell element. Geometrical description

where  $\tilde{\epsilon}_{ij}$  are the covariant components of the strain tensor measured in the natural coordinate system and  $\underline{\mathbf{g}}^i$  are the contravariant base vectors (In Eqn. (10)  $\underline{\mathbf{g}}^i \underline{\mathbf{g}}^j$  indicates a tensorial product between the two vectors, some Authors use the notation  $\underline{\mathbf{g}}^i \otimes \underline{\mathbf{g}}^j$ ).

In the MITC4 formulation we selected the following strain interpolations:

- The “in-layer” strain components ( $\tilde{\epsilon}_{11}, \tilde{\epsilon}_{22}, \tilde{\epsilon}_{12}$ ) are directly calculated from the displacement / rotation interpolations.
- The transverse shear strains ( $\tilde{\epsilon}_{13}, \tilde{\epsilon}_{23}$ ) are interpolated using the following functions (see Fig. 5)

$$\tilde{\epsilon}_{13} = \frac{1}{2} (1 + r_2) \tilde{\epsilon}_{13}|_A^{DI} + \frac{1}{2} (1 - r_2) \tilde{\epsilon}_{13}|_C^{DI} \quad (11.a)$$

$$\tilde{\epsilon}_{23} = \frac{1}{2} (1 + r_1) \tilde{\epsilon}_{23}|_D^{DI} + \frac{1}{2} (1 - r_1) \tilde{\epsilon}_{23}|_B^{DI} \quad (11.b)$$

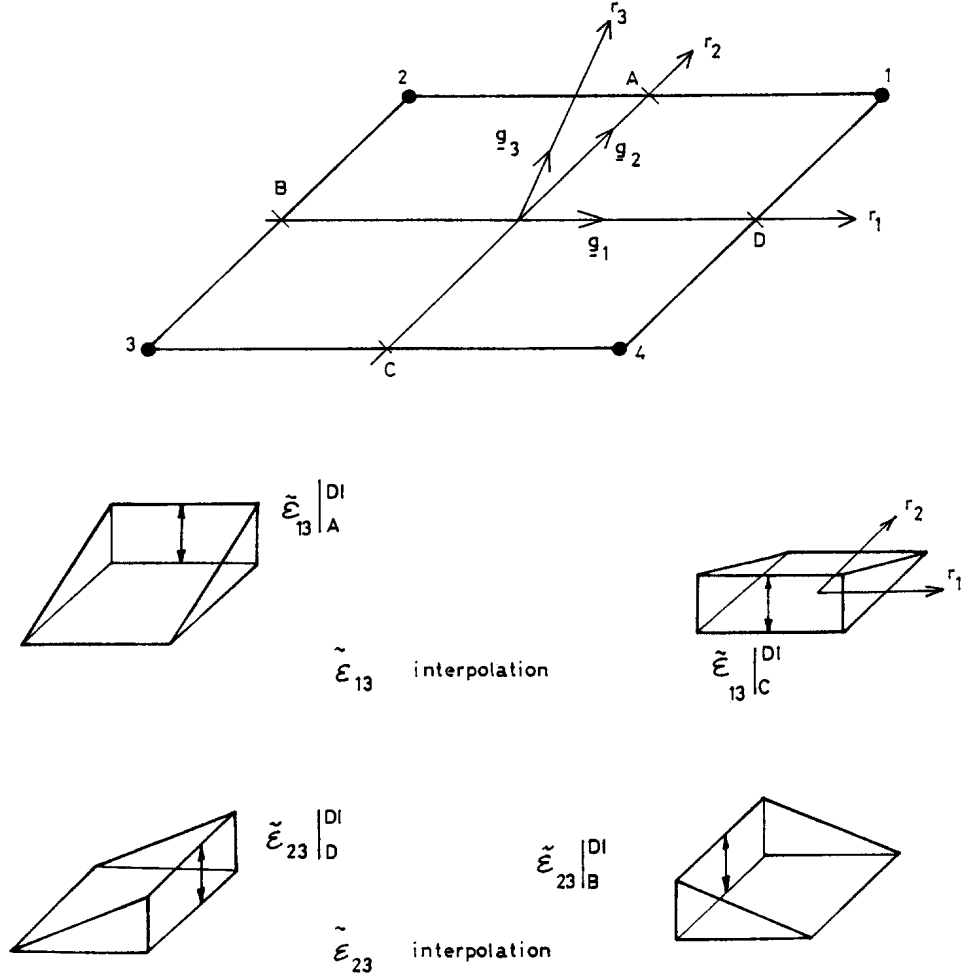


Figure 5. MITC4 shell element. Transverse shear strains interpolation

In the above equations we indicate with the notation  $\tilde{\epsilon}_{ij}|_P^{DI}$  the covariant strain components calculated at the *sampling point* P from the displacement/rotation interpolations.

Equations (11) provide non-compatible shear strains, therefore Irons' Patch Test will have to be satisfied in order to assure the element convergence [2,22].

At any point inside the element a local Cartesian system with base vectors  $\hat{\mathbf{e}}_i (i = 1, 2, 3)$  is defined as shown in Figure 6. In the local Cartesian system the constitutive fourth-order tensor  $\underline{\underline{\mathbf{C}}}$  is defined by degenerating the 3D constitutive tensor to impose the simultaneous satisfaction of

$$\hat{\sigma}_{33} = 0 \quad (12.a)$$

$$\hat{\epsilon}_{33} = 0 \quad (12.b)$$

see Ref. [6] for details.

In the natural coordinate system

$$\tilde{C}^{ijkl} = (\underline{\mathbf{g}}^i \cdot \hat{\mathbf{e}}_m) (\underline{\mathbf{g}}^j \cdot \hat{\mathbf{e}}_n) (\underline{\mathbf{g}}^k \cdot \hat{\mathbf{e}}_o) (\underline{\mathbf{g}}^l \cdot \hat{\mathbf{e}}_p) \hat{C}^{mnop} \quad (13)$$

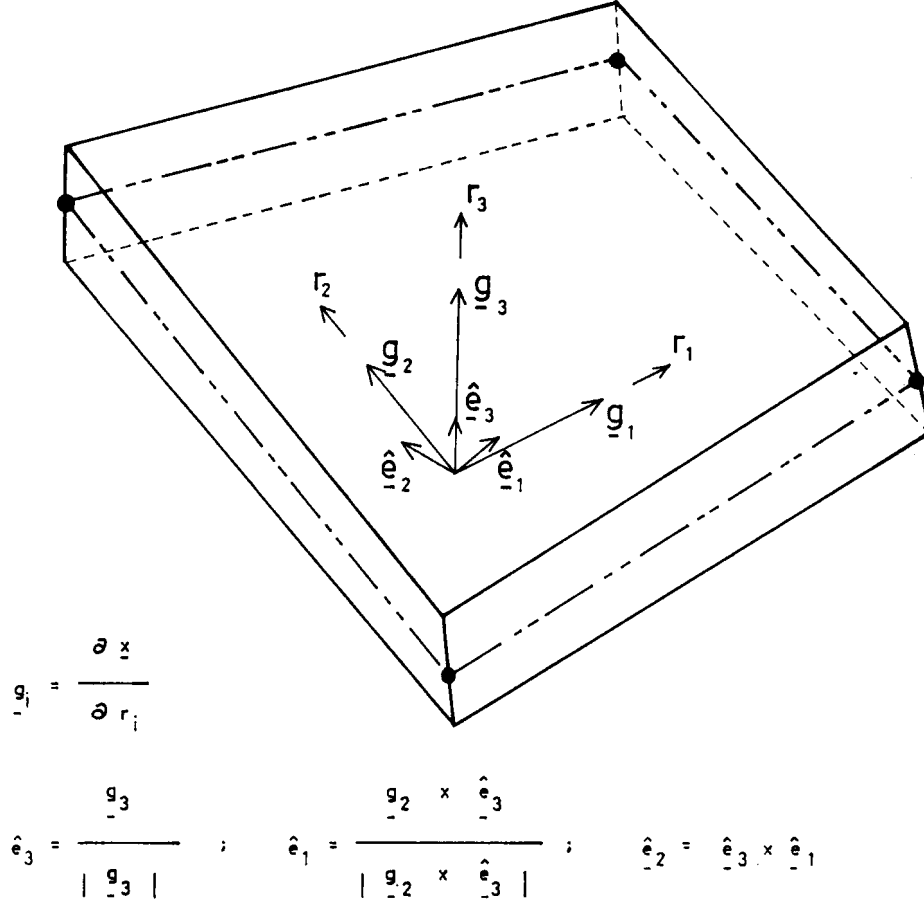


Figure 6. Local Cartesian system

hence

$$\tilde{\sigma}^{ij} = \tilde{C}^{ijkl} \tilde{\epsilon}_{kl} \quad (14)$$

where  $\underline{\underline{\sigma}}$  is the Cauchy stress tensor.

In order to assure the *convergence* of the MITC4 formulation two issues have to be analyzed: the stability and the consistency of the formulation [24].

Regarding the *stability* issue the eigenvalues of the stiffness matrices of undistorted and distorted elements were examined. In all cases, as expected, the elements presented only the six rigid body modes and no spurious rigid body modes [9,10].

In order to check the *consistency* of the formulation the Patch Tests shown in Figure 7 were performed. In all cases the transverse displacements, rotations and stresses exactly agreed with the analytical results [9,10]. An analytical proof that the MITC4 satisfies the bending Patch Test was presented in our Ref. [12].

Finally it should be noted that the Patch Test is obviously passed by the three possible membrane loadings.

We have already published extensive numerical experimentation illustrating on the MITC4 performance in linear analyses [9-13]. In Figures 8 to 10 we reproduce the results corresponding to a few selected linear benchmark cases.

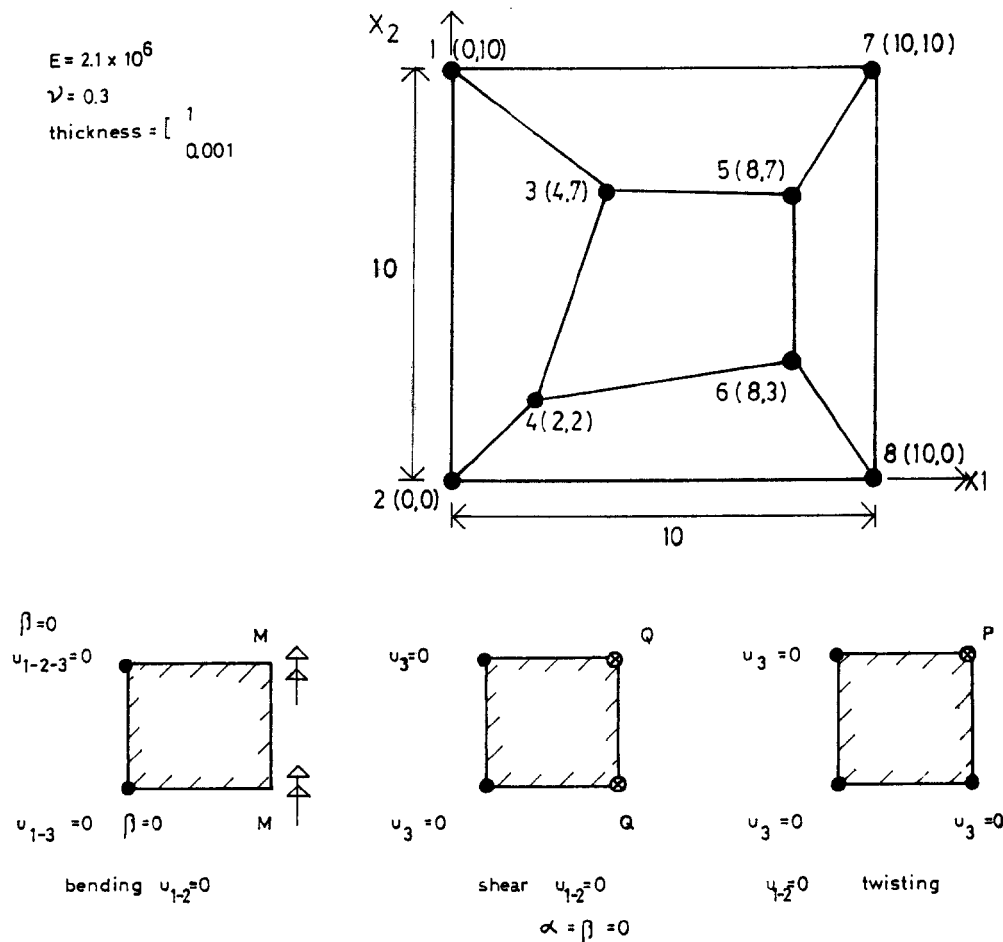


Figure 7. MITC4 shell element. Patch tests

### 3.2 The MITC8 shell element

The eight-node MITC8 shell element formulation was designed so as to fulfil the following reliability criteria [12-13]:

- The element should not present either shear locking or membrane locking.
- The element should not contain spurious rigid body modes.
- The element should satisfy Irons' Patch Test.
- The element should have low sensitivity to distortions.

The geometrical description and kinematics of the element (displacement/rotation interpolations) are the ones corresponding to the eight-node standard A-I-Z shell element (see Eqns. (1) to (3) and Figures 11.a and 11.b).

The strain tensor at any point inside the element is written in the natural coordinate system of the element as:

$$\underline{\underline{\epsilon}} = \underbrace{\tilde{\epsilon}_{rr} \mathbf{g}^r \mathbf{g}^r + \tilde{\epsilon}_{ss} \mathbf{g}^s \mathbf{g}^s + \tilde{\epsilon}_{rs} (\mathbf{g}^r \mathbf{g}^s + \mathbf{g}^s \mathbf{g}^r)}_{\text{in-layer strains}} + \underbrace{\tilde{\epsilon}_{rt} (\mathbf{g}^r \mathbf{g}^t + \mathbf{g}^t \mathbf{g}^r) + \tilde{\epsilon}_{st} (\mathbf{g}^s \mathbf{g}^t + \mathbf{g}^t \mathbf{g}^s)}_{\text{transverse strains}} \quad (15)$$

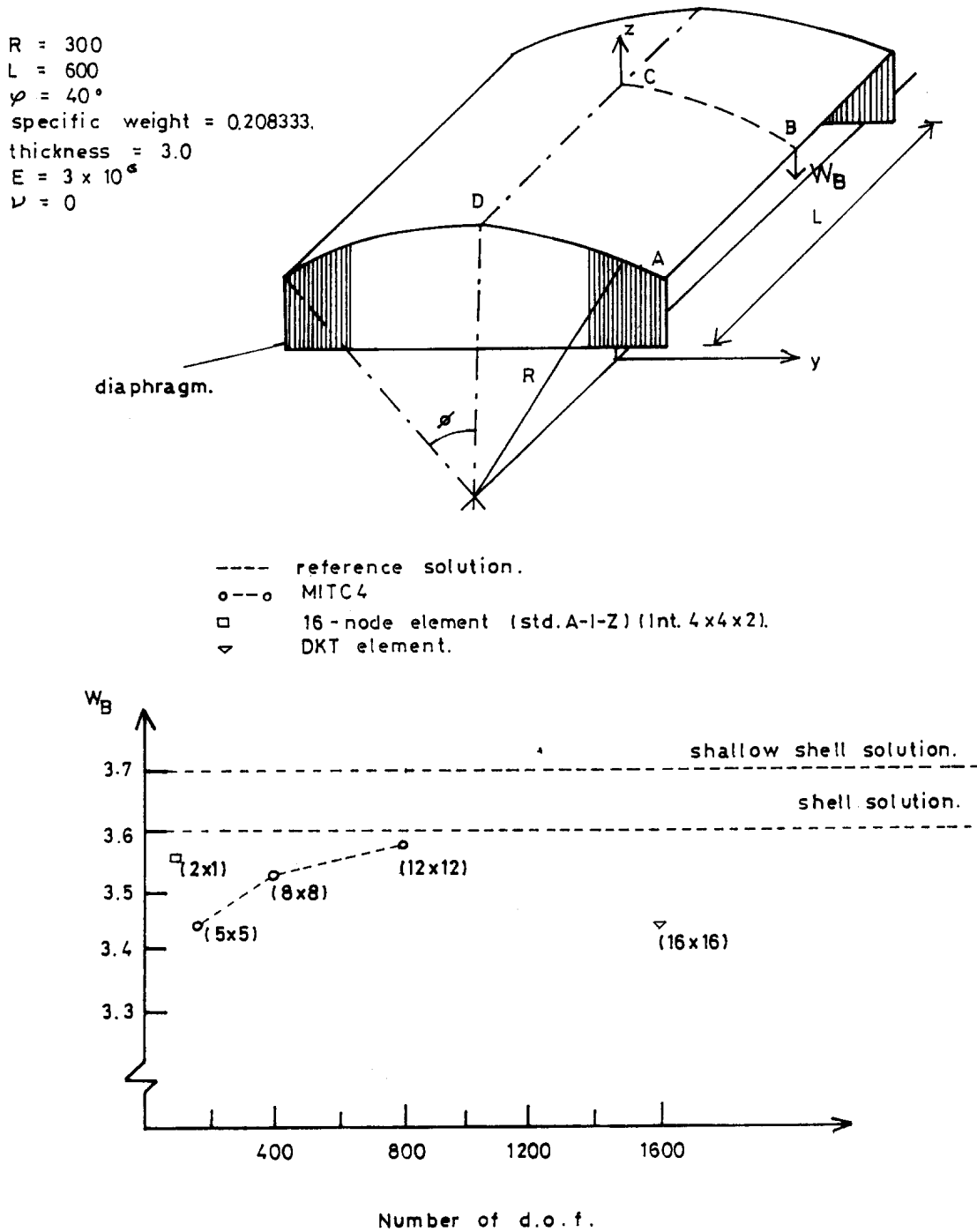
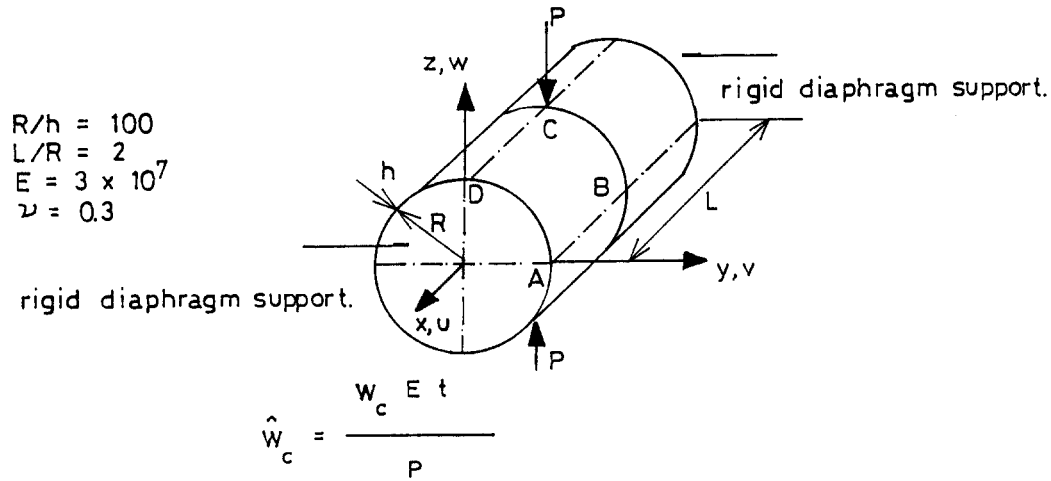


Figure 8. Scordelis-Lo shell (MITC4)

In the MITC8 shell element formulation we use special interpolations for the in-layer and transverse shear strains.



$\hat{W}_c$  series solution = -164.24 by Lindberg et.al.

MESH FOR 1/8 TH OF SHELL	NUMBER OF D.O.F.	$\hat{W}_c^{FEM} / \hat{W}_c^{ANALYT.}$
5 x 5	130	0.51
10 x 10	510	0.83
20 x 20	2020	0.96

a) Convergence study for MITC4 element.

ELEMENT	MESH FOR 1/8 TH OF SHELL.	NUMBER OF D.O.F.	$\hat{W}_c^{FEM} / \hat{W}_c^{ANALYT.}$
MITC 4	20 x 20	2020	0.96
16-NODE std. AIZ	10 x 10	4530	0.98

b) Comparison between MITC4 and 16-node (Std.A-I-Z) elements.

Figure 9. Pinched cylinder (MITC4)

### 3.2.1 In-layer strain interpolation

To avoid membrane locking and obtain an element formulation that does not contain spurious rigid body modes we use the following in-layer strains interpolation (see Fig. 11.c)

$$\underline{\epsilon}^{ILS} = \sum_{i=1}^8 h_i^{ILS} \underline{\epsilon}_i^{ILS} \tag{16.a}$$

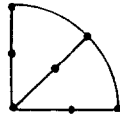
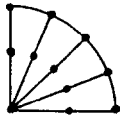
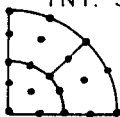
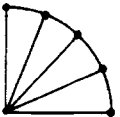
	F. E. M. MODEL	$ \epsilon_W  = \frac{ WFE - WAN }{ WAN }$	$\epsilon_\tau = \frac{ \tau_{PP}^{max} }{ E\alpha\theta }$
S T A N D A R D  A-I-Z  E L E M E N T S		0.26	1.10
		0.07	0.54
	INT. 3x3x2 	0.008	CENTRAL ELEM. 0.62
	SAME MODEL INT. 2x2x2	0.014	OUTER ELEM. 0.22
	INT. 4x4x2 	0.003	0.26
	SAME MODEL INT. 3x3x2	0.0001	0.04
MITC 4	INT. 2x2x2 	0	0

Figure 10. Circular plate with constant temperature gradient through the thickness (MITC4)

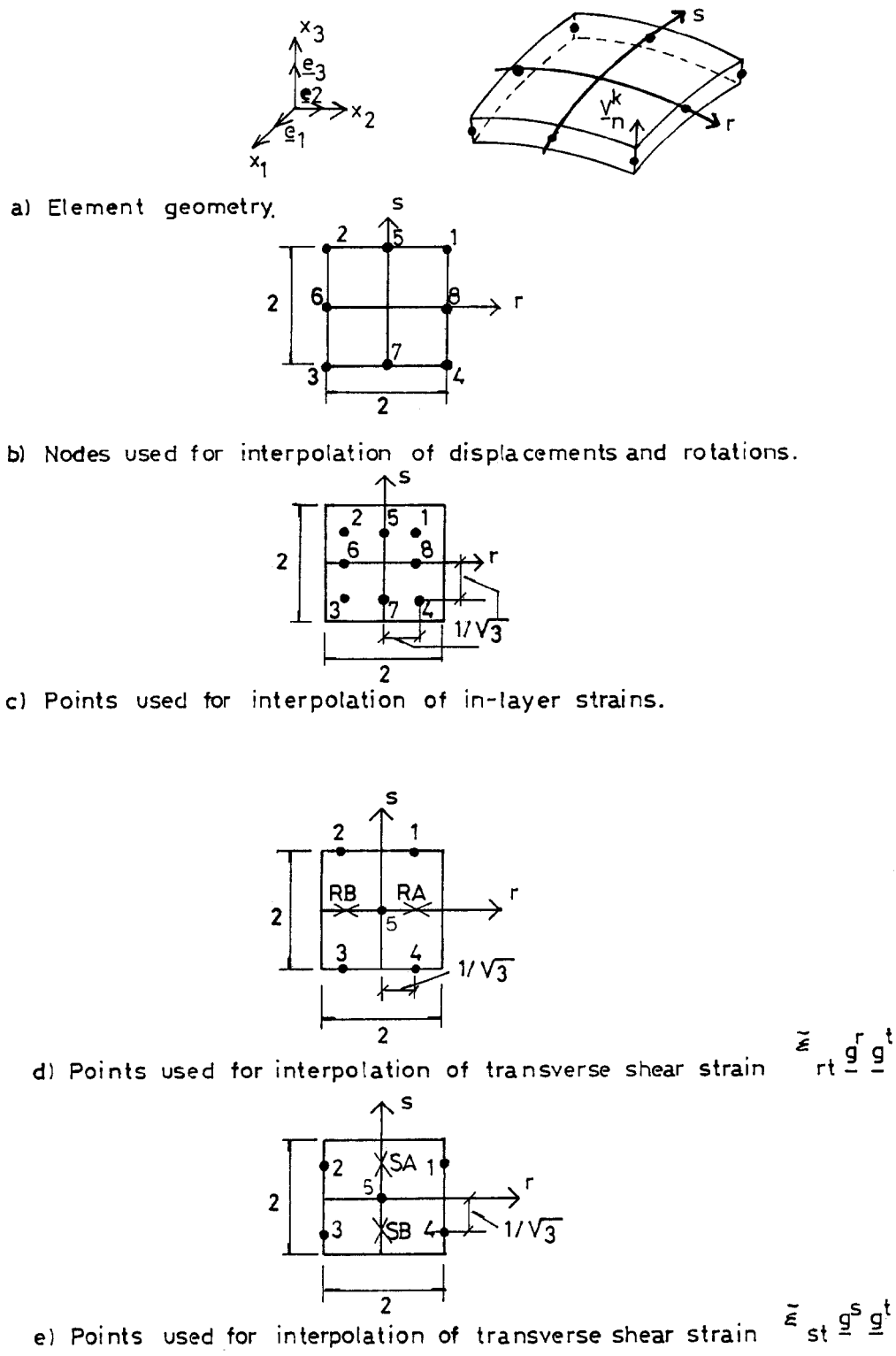


Figure 11. (MITC8) shell element

The interpolation functions  $h_i^{ILS}$  are obtained from the classical serendipity interpolation functions for a square domain ( $-1 \leq r, s \leq 1$ ) [2,6] by replacing the variables “ $r$ ” and “ $s$ ” with “ $r \setminus a$ ” and “ $s \setminus a$ ” respectively, where  $a = \frac{1}{\sqrt{3}}$ .

For  $i = 1$  to 4 we use

$$\underline{\underline{\mathfrak{E}}}_i^{ILS} = \tilde{\epsilon}_{rr} \underline{\underline{\mathfrak{g}}}^r \underline{\underline{\mathfrak{g}}}^r |_i^{DI} + \tilde{\epsilon}_{ss} \underline{\underline{\mathfrak{g}}}^s \underline{\underline{\mathfrak{g}}}^s |_i^{DI} + \tilde{\epsilon}_{rs} (\underline{\underline{\mathfrak{g}}}^r \underline{\underline{\mathfrak{g}}}^s + \underline{\underline{\mathfrak{g}}}^s \underline{\underline{\mathfrak{g}}}^r) |_i^{DI} \quad (16.b)$$

where  $\tilde{\epsilon}_{lm} \underline{\underline{\mathfrak{g}}}^l \underline{\underline{\mathfrak{g}}}^m |_i^{DI}$  is directly calculated from the geometry and kinematics interpolation at the  $i$ -th sampling point (Fig. 11.c).

For  $i = 5$  and  $i = 7$  we use

$$\underline{\underline{\mathfrak{E}}}_5^{ILS} = \tilde{\epsilon}_{ss} \underline{\underline{\mathfrak{g}}}^s \underline{\underline{\mathfrak{g}}}^s |_5^{DI} + \left\{ \underline{\underline{\mathfrak{g}}}_r \cdot \left[ \frac{1}{2} (\underline{\underline{\mathfrak{E}}}_1^{DI} + \underline{\underline{\mathfrak{E}}}_2^{DI}) \right] \cdot \underline{\underline{\mathfrak{g}}}_r \right\} \underline{\underline{\mathfrak{g}}}_r \underline{\underline{\mathfrak{g}}}_r |_5^{DI} + \left\{ \underline{\underline{\mathfrak{g}}}_r \cdot \left[ \frac{1}{2} (\underline{\underline{\mathfrak{E}}}_1^{DI} + \underline{\underline{\mathfrak{E}}}_2^{DI}) \right] \cdot \underline{\underline{\mathfrak{g}}}_s \right\} (\underline{\underline{\mathfrak{g}}}_r \underline{\underline{\mathfrak{g}}}_s + \underline{\underline{\mathfrak{g}}}_s \underline{\underline{\mathfrak{g}}}_r) |_5^{DI} \quad (16.c)$$

$$\underline{\underline{\mathfrak{E}}}_7^{ILS} = \tilde{\epsilon}_{ss} \underline{\underline{\mathfrak{g}}}^s \underline{\underline{\mathfrak{g}}}^s |_7^{DI} + \left\{ \underline{\underline{\mathfrak{g}}}_r \cdot \left[ \frac{1}{2} (\underline{\underline{\mathfrak{E}}}_3^{DI} + \underline{\underline{\mathfrak{E}}}_4^{DI}) \right] \cdot \underline{\underline{\mathfrak{g}}}_r \right\} \underline{\underline{\mathfrak{g}}}_r \underline{\underline{\mathfrak{g}}}_r |_7^{DI} + \left\{ \underline{\underline{\mathfrak{g}}}_r \cdot \left[ \frac{1}{2} (\underline{\underline{\mathfrak{E}}}_3^{DI} + \underline{\underline{\mathfrak{E}}}_4^{DI}) \right] \cdot \underline{\underline{\mathfrak{g}}}_s \right\} (\underline{\underline{\mathfrak{g}}}_r \underline{\underline{\mathfrak{g}}}_s + \underline{\underline{\mathfrak{g}}}_s \underline{\underline{\mathfrak{g}}}_r) |_7^{DI} \quad (16.d)$$

where

$$\underline{\underline{\mathfrak{g}}}_s \equiv \underline{\underline{\mathfrak{g}}}_s \quad ; \quad \underline{\underline{\mathfrak{g}}}_t \equiv \underline{\underline{\mathfrak{g}}}_t \quad ; \quad \underline{\underline{\mathfrak{g}}}_r = \underline{\underline{\mathfrak{g}}}_r - \alpha \underline{\underline{\mathfrak{g}}}_s \quad ; \quad \alpha = \frac{g_{rs}}{g_{ss}} \quad (16.e)$$

For  $i = 6$  and  $i = 8$  we use

$$\underline{\underline{\mathfrak{E}}}_6^{ILS} = \tilde{\epsilon}_{rr} \underline{\underline{\mathfrak{g}}}_r \underline{\underline{\mathfrak{g}}}_r |_6^{DI} + \left\{ \underline{\underline{\mathfrak{g}}}_s \cdot \left[ \frac{1}{2} (\underline{\underline{\mathfrak{E}}}_2^{DI} + \underline{\underline{\mathfrak{E}}}_3^{DI}) \right] \cdot \underline{\underline{\mathfrak{g}}}_s \right\} \underline{\underline{\mathfrak{g}}}_s \underline{\underline{\mathfrak{g}}}_s |_6^{DI} + \left\{ \underline{\underline{\mathfrak{g}}}_r \cdot \left[ \frac{1}{2} (\underline{\underline{\mathfrak{E}}}_2^{DI} + \underline{\underline{\mathfrak{E}}}_3^{DI}) \right] \cdot \underline{\underline{\mathfrak{g}}}_s \right\} (\underline{\underline{\mathfrak{g}}}_r \underline{\underline{\mathfrak{g}}}_s + \underline{\underline{\mathfrak{g}}}_s \underline{\underline{\mathfrak{g}}}_r) |_6^{DI} \quad (16.f)$$

$$\underline{\underline{\mathfrak{E}}}_8^{ILS} = \tilde{\epsilon}_{rr} \underline{\underline{\mathfrak{g}}}_r \underline{\underline{\mathfrak{g}}}_r |_8^{DI} + \left\{ \underline{\underline{\mathfrak{g}}}_s \cdot \left[ \frac{1}{2} (\underline{\underline{\mathfrak{E}}}_1^{DI} + \underline{\underline{\mathfrak{E}}}_4^{DI}) \right] \cdot \underline{\underline{\mathfrak{g}}}_s \right\} \underline{\underline{\mathfrak{g}}}_s \underline{\underline{\mathfrak{g}}}_s |_8^{DI} + \left\{ \underline{\underline{\mathfrak{g}}}_r \cdot \left[ \frac{1}{2} (\underline{\underline{\mathfrak{E}}}_1^{DI} + \underline{\underline{\mathfrak{E}}}_4^{DI}) \right] \cdot \underline{\underline{\mathfrak{g}}}_s \right\} (\underline{\underline{\mathfrak{g}}}_r \underline{\underline{\mathfrak{g}}}_s + \underline{\underline{\mathfrak{g}}}_s \underline{\underline{\mathfrak{g}}}_r) |_8^{DI} \quad (16.g)$$

where

$$\underline{\underline{\mathfrak{g}}}_r \equiv \underline{\underline{\mathfrak{g}}}_r \quad ; \quad \underline{\underline{\mathfrak{g}}}_t \equiv \underline{\underline{\mathfrak{g}}}_t \quad ; \quad \underline{\underline{\mathfrak{g}}}_s = \underline{\underline{\mathfrak{g}}}_s - \beta \underline{\underline{\mathfrak{g}}}_r \quad ; \quad \beta = \frac{g_{rs}}{g_{rr}} \quad (16.h)$$

### 3.2.2 Transverse shear strain interpolations

To avoid shear locking and obtain an element formulation that does not contain spurious rigid body modes we use the following interpolations for the transverse shear strains (Figs. 11.d and 11.e).

$$\tilde{\varepsilon}_{rt} \underline{\mathbf{g}}^r \underline{\mathbf{g}}^t = \sum_{i=1}^4 h_i^{RT} \tilde{\varepsilon}_{rt} \underline{\mathbf{g}}^r \underline{\mathbf{g}}^t|_i^{DI} + h_5^{RT} (\tilde{\varepsilon}_{rt}|_{RA}^{DI} + \tilde{\varepsilon}_{rt}|_{RB}^{DI}) \underline{\mathbf{g}}^r \underline{\mathbf{g}}^t|_5^{DI} \quad (17)$$

where

$$\begin{aligned} h_1^{RT} &= \frac{1}{4} \left[ 1 + \frac{r}{a} \right] (1+s) - \frac{1}{4} h_5^{RT} \\ h_2^{RT} &= \frac{1}{4} \left[ 1 - \frac{r}{a} \right] (1+s) - \frac{1}{4} h_5^{RT} \\ h_3^{RT} &= \frac{1}{4} \left[ 1 - \frac{r}{a} \right] (1-s) - \frac{1}{4} h_5^{RT} \\ h_4^{RT} &= \frac{1}{4} \left[ 1 + \frac{r}{a} \right] (1-s) - \frac{1}{4} h_5^{RT} \\ h_5^{RT} &= \left[ 1 - \left( \frac{r}{a} \right)^2 \right] (1-s^2) \end{aligned} \quad (18)$$

In the above  $a = \frac{1}{\sqrt{3}}$ .

Similarly

$$\tilde{\varepsilon}_{st} \underline{\mathbf{g}}^s \underline{\mathbf{g}}^t = \sum_{i=1}^4 h_i^{ST} \tilde{\varepsilon}_{st} \underline{\mathbf{g}}^s \underline{\mathbf{g}}^t|_i^{DI} + h_5^{ST} \left[ \frac{1}{2} (\tilde{\varepsilon}_{st}|_{SA}^{DI} + \tilde{\varepsilon}_{st}|_{SB}^{DI}) \right] \underline{\mathbf{g}}^s \underline{\mathbf{g}}^t|_5^{DI} \quad (19)$$

The functions  $h_i^{ST}$  are obtained from Eqns. (18) replacing  $r$  by  $s$  and viceversa.

In order to assure the *convergence* of the MITC8 formulation two issues have to be analyzed: the stability and the consistency of the formulation [24].

Regarding *stability* we have shown that the MITC8 shell element formulation does not contain spurious rigid body modes.

However, regarding the *consistency* of the formulation, we can only assess that when using elements with straight sides and evenly spaced nodes the Patch Tests are all exactly satisfied. Relatively small errors arise in the Patch Test results obtained using elements with curved sides or with mid-side nodes not placed at their mid-side physical location.

We have already published extensive numerical experimentation illustrating on the MITC8 performance in linear analyses [12-13]. In Figures 12 to 16 we reproduce the results corresponding to a few selected linear benchmark cases.

## 4. GEOMETRIC AND MATERIAL NONLINEAR FORMULATIONS (SMALL STRAINS)

We formulate an incremental analysis: being known the configuration at time (load level)  $t$  we search for the configuration at time (load level)  $t + \Delta t$  [6]. For this purpose we make use of the Total Lagrangian Formulation [6].

For the equilibrium configuration at time  $t + \Delta t$  the Principle of Virtual Work [6], states

$$\int_{\circ V} {}^{t+\Delta t} \underline{\mathbf{S}} : \delta ({}^{t+\Delta t} \underline{\boldsymbol{\varepsilon}}) \circ dV = {}^{t+\Delta t} \mathfrak{R} \quad (20)$$

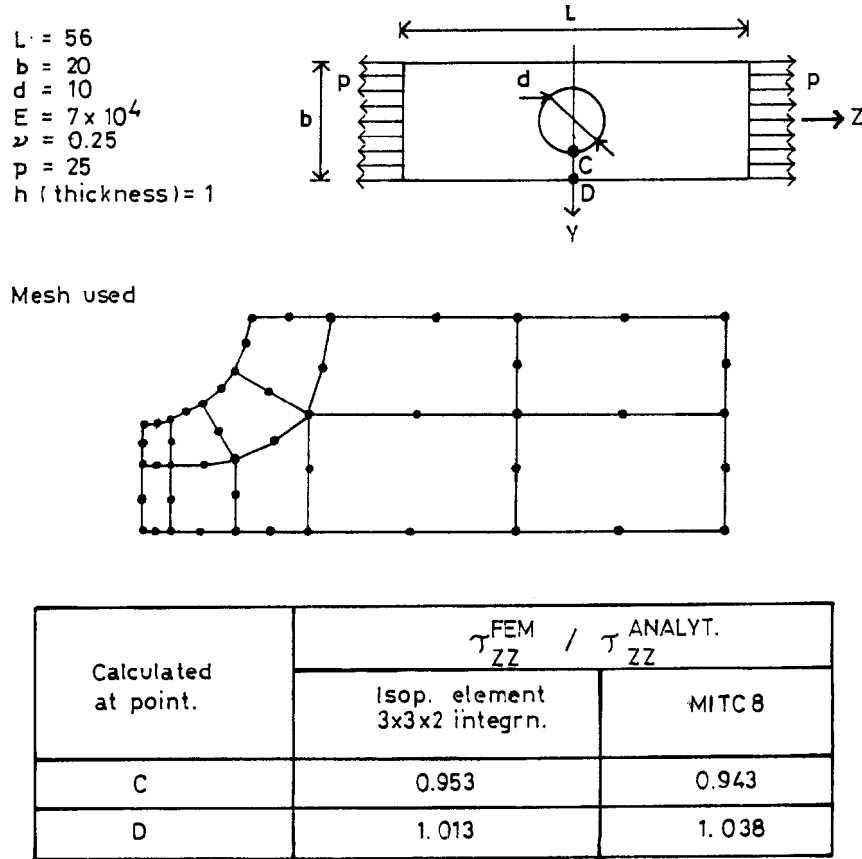


Figure 12. Analysis of a plane stress perforated plate (MITC8)

In the above we have used Bathe's notation and:

- ${}^t\underline{\underline{\mathbf{S}}}$ : 2nd. Piola-Kirchhoff stress tensor, corresponding to the  $t$ -configuration and referred to the configuration at time  $t = 0$  (undeformed) [25-28]. It should be remembered that  ${}^t\underline{\underline{\mathbf{S}}}$  is the pull-back of the Kirchhoff stress tensor ( ${}^t\underline{\underline{\mathbf{T}}}$ ) from the  $t$ -configuration to the configuration at  $t = 0$  [25,26].

Defining a coordinate system in the  $t$ -configuration (spatial configuration), with coordinates  $\{t x^i ; i = 1, 2, 3\}$  and covariant base vectors  ${}^t\underline{\underline{\mathbf{g}}}_i$ , we can write

$${}^t\underline{\underline{\mathbf{T}}} = {}^t\tau^{ij} {}^t\underline{\underline{\mathbf{g}}}_i {}^t\underline{\underline{\mathbf{g}}}_j \quad (21.a)$$

where

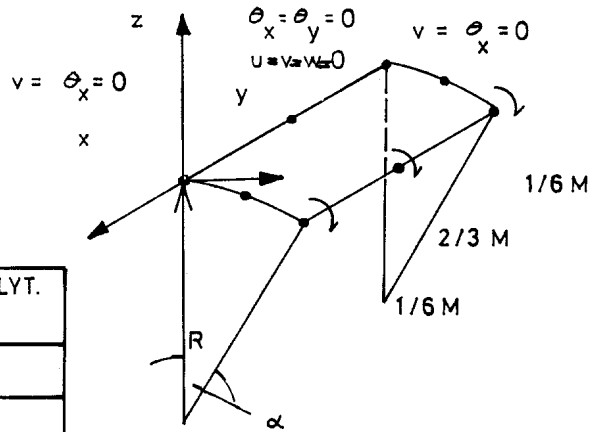
$${}^t\tau^{ij} = \frac{{}^\circ\rho}{{}^t\rho} {}^t\sigma^{ij} \quad (21.b)$$

${}^\circ\rho, {}^t\rho$ : densities in the  $t = 0$  and  $t$ -configurations respectively.

${}^t\sigma^{ij}$ : contravariant components of the Cauchy stress tensor in the spatial configuration. Defining a coordinate system in the configuration corresponding to  $t = 0$  (reference configuration), with coordinates  $\{X^I ; I = 1, 2, 3\}$  and covariant base vectors  $\underline{\underline{\mathbf{G}}}_I$ , we can write

$${}^t\underline{\underline{\mathbf{S}}} = {}^tS^{IJ} \underline{\underline{\mathbf{G}}}_I \underline{\underline{\mathbf{G}}}_J \quad (22.a)$$

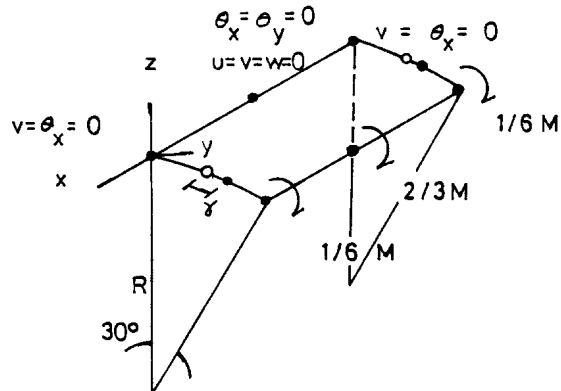
$R = 20$   
 $h$  (thickness) = 0.2  
 $E = 2.1 \times 10^6$   
 $\nu = 0.3$



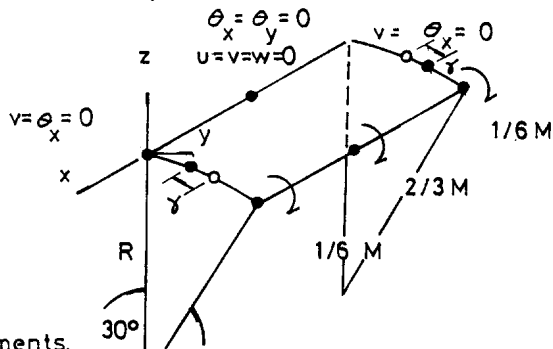
$\alpha$ [degrees]	$\theta^{FEM} / \theta^{ANALYT.}$
30	0.999
60	0.994
90	0.981

a) Results using undistorted element.

$\gamma$ [degrees]	$\theta^{FEM} / \theta^{ANALYT.}$
0	0.999
3	1.000
5	1.001



$\gamma$ [degrees]	$\theta^{FEM} / \theta^{ANALYT.}$
0	0.999
3	0.974
5	0.928



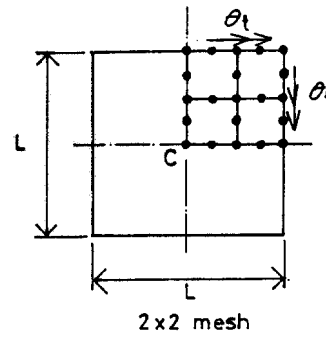
b) Results using distorted elements.

Figure 13. The MITC8 shell element does not lock

$L = 20$   
 thickness = 0.02  
 $E = 2.1 \times 10^6$   
 $\nu = 0.3$

Boundary conditions

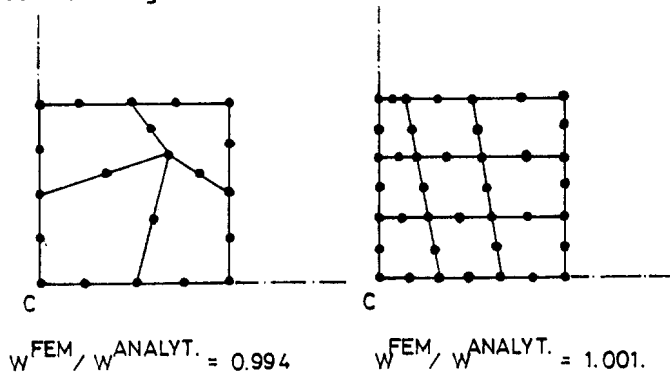
- Simply supported edge  $w=0$
- Clamped edge  $w=0$   
 $\theta_t=0$



$\frac{W^{FEM}}{W^{ANALYT.}}$ FOR SIMPLY SUPPORTED PLATE AT C.		
ME SH	Uniform Pressure	Concentrated Load
1 x 1	0.993	1.003
2 x 2	1.000	0.998
3 x 3	1.000	0.999

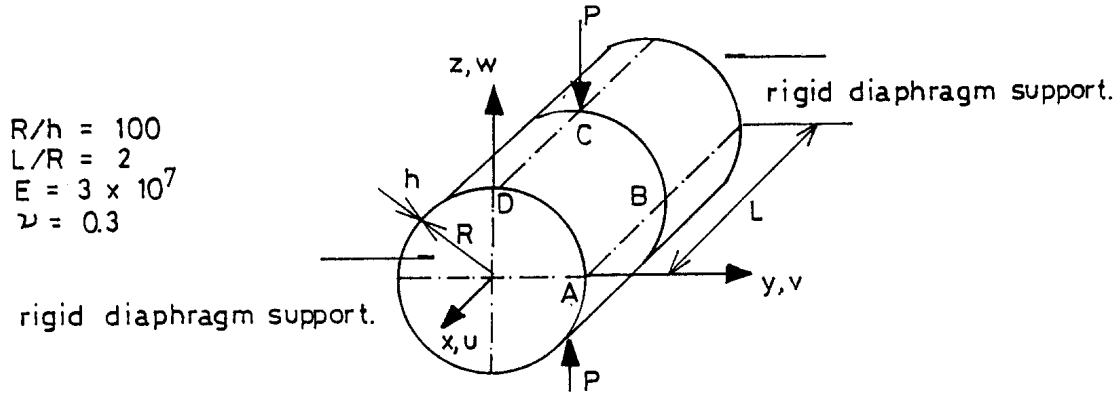
$\frac{W^{FEM}}{W^{ANALYT.}}$ FOR CLAMPED PLATE AT C.		
ME SH	Uniform Pressure	Concentrated Load
1 x 1	1.240	1.118
2 x 2	1.005	1.000
3 x 3	1.005	1.001

a) Results using undistorted elements.



b) Results using distorted elements, case of simply supported plate and uniform pressure.

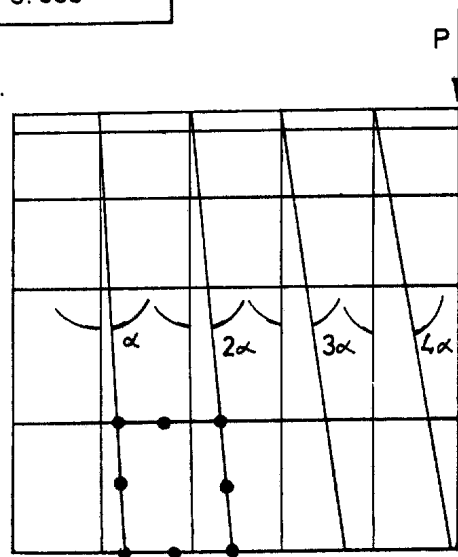
Figure 14. Analysis of plates (MITC8)



MESH FOR ABCD	$W_C^{FEM} / W_C^{ANALYT.}$
3 x 3	0.833
5 x 5	0.952
8 x 8	0.990
10 x 10	0.999

a) Results using undistorted elements.

$\alpha$ [degrees]	$W_C^{FEM} / W_C^{ANALYT.}$
0	0.952
1	0.951
1 1/2	0.950
2	0.949
2 1/2	0.949



b) Results using distorted elements (5x5 mesh)

Figure 15. Pinched cylinder (MITC8)



In the spatial configuration

$$\underline{\underline{\sigma}}^t = {}^t\tilde{\sigma}^{ij} \underline{\underline{\mathbf{g}}}_i^t \underline{\underline{\mathbf{g}}}_j^t \quad (25.a)$$

$$\underline{\underline{\tau}}^t = {}^t\tilde{\tau}^{ij} \underline{\underline{\mathbf{g}}}_i^t \underline{\underline{\mathbf{g}}}_j^t \quad (25.b)$$

$$\underline{\underline{\mathbf{e}}}^t = {}^t\tilde{e}_{ij} \underline{\underline{\mathbf{g}}}_i^t \underline{\underline{\mathbf{g}}}_j^t \quad (25.c)$$

and in the reference configuration

$$\underline{\underline{\mathbf{S}}}^t = {}^t\tilde{S}^{IJ} \underline{\underline{\mathbf{G}}}_I^t \underline{\underline{\mathbf{G}}}_J^t \quad (26.a)$$

$$\underline{\underline{\mathbf{E}}}^t = {}^t\tilde{E}_{IJ} \underline{\underline{\mathbf{G}}}_I^t \underline{\underline{\mathbf{G}}}_J^t \quad (26.b)$$

It is worth pointing out that [26]

$${}^t\tilde{S}^{IJ} = {}^t\tilde{\tau}^{ij} \quad (27.a)$$

$${}^t\tilde{E}_{IJ} = {}^t\tilde{e}_{ij} \quad (27.b)$$

for  $I = i$  and  $J = j$ .

For the incremental step from the  $t$ -configuration to the  $(t + \Delta t)$ -configuration [6]

$${}^{t+\Delta t}\tilde{S}^{IJ} = {}^t\tilde{S}^{IJ} + \underbrace{{}^t\tilde{S}^{IJ}}_{\text{increment}} \quad (28.a)$$

$${}^{t+\Delta t}\tilde{E}_{IJ} = {}^t\tilde{E}_{IJ} + \underbrace{{}^t\tilde{E}_{IJ}}_{\text{increment}} \quad (28.b)$$

$${}^t\tilde{E}_{IJ} = \underbrace{{}^t\tilde{E}_{IJ}}_{\text{linear terms}} + \underbrace{{}^t\tilde{\eta}_{IJ}}_{\text{nonlinear terms}} \quad (28.c)$$

For linearizing the step we use [6]

$${}^t\tilde{S}^{IJ} = {}^t\tilde{C}^{IJKL} {}^t\tilde{e}_{KL} \quad (29.a)$$

$$\delta {}^t\tilde{E}_{IJ} = \delta {}^t\tilde{e}_{IJ} \quad (29.b)$$

In Eqn. (29.a)  ${}^t\tilde{\underline{\underline{\mathbf{C}}}}$  is the tangent constitutive tensor [29-31] in the reference configuration [25-26].

Hence, the *linearized incremental equations* are [6]

$$\int_{{}^t\mathcal{V}} {}^t\tilde{C}^{IJKL} {}^t\tilde{e}_{KL} \delta ({}^t\tilde{e}_{IJ}) \, {}^t\text{d}V + \int_{{}^t\mathcal{V}} {}^t\tilde{S}^{IJ} \delta ({}^t\tilde{\eta}_{IJ}) \, {}^t\text{d}V = {}^{t+\Delta t}\mathfrak{R} - \int_{{}^t\mathcal{V}} {}^t\tilde{S}^{IJ} \delta ({}^t\tilde{e}_{IJ}) \, {}^t\text{d}V \quad (30)$$

As it is well known, the  $(t + \Delta t)$ -configuration is determined using the above equation in an iterative scheme [6,32,33].

As this point it is important to recognize that in a geometrically nonlinear analysis we are dealing with *finite rotations* that cannot be considered vectors anymore [34].

#### 4.1 Finite rotations formulation

In this Section we will revise the A-I-Z shell element formulation for the case of finite rotations, following our previous work in Ref. [34].

In the step from  $t$  to  $t + \Delta t$ , at any node “ $k$ ”

$${}^{t+\Delta t}\underline{\mathbf{V}}_n^k = {}^{t+\Delta t}\underline{\underline{\mathbf{R}}}^k \cdot {}^t\underline{\mathbf{V}}_n^k \quad (31)$$

where  ${}^{t+\Delta t}\underline{\underline{\mathbf{R}}}^k$  is a rotation tensor and  $|{}^t\underline{\mathbf{V}}_n^k| = |{}^{t+\Delta t}\underline{\mathbf{V}}_n^k| = 1$ .

It is obvious that the rotation defined in Eqn. (31) is a rotation around an axis normal to the plane  $({}^t\underline{\mathbf{V}}_n^k, {}^{t+\Delta t}\underline{\mathbf{V}}_n^k)$ . Therefore the rotation axis is contained in the plane  $({}^t\underline{\mathbf{V}}_1^k, {}^t\underline{\mathbf{V}}_2^k)$ .

Following Argyris [35] we can write the rotation tensor  ${}^{t+\Delta t}\underline{\underline{\mathbf{R}}}^k$  in a Cartesian system with orthonormal base vectors  $({}^t\underline{\mathbf{V}}_1^k, {}^t\underline{\mathbf{V}}_2^k, {}^t\underline{\mathbf{V}}_n^k)$ ; in this system, the matrix formed with the rotation tensor components is

$$[{}^{t+\Delta t}R^k] = [I_3] + \frac{\sin(\theta^k)}{\theta^k} [\Theta^k] + \frac{1}{2} \left[ \frac{\sin(\theta^k/2)}{(\theta^k/2)} \right]^2 [\Theta^k]^2 \quad (32.a)$$

In the above

$$\theta^k = [(\theta_1^k)^2 + (\theta_2^k)^2]^{\frac{1}{2}} \quad (32.b)$$

$$[\Theta^k] = \begin{bmatrix} 0 & 0 & \theta_2^k \\ 0 & 0 & -\theta_1^k \\ -\theta_2^k & \theta_1^k & 0 \end{bmatrix} \quad (32.c)$$

$[I_3]$  is a unit (3x3) matrix.

It is important to note that

- For infinitesimal incremental rotations  $\theta_1^k$  and  $\theta_2^k$  are independent infinitesimal rotations around  ${}^t\underline{\mathbf{V}}_1^k$  and  ${}^t\underline{\mathbf{V}}_2^k$  respectively.
- For finite incremental rotations  $\theta_1^k$  and  $\theta_2^k$  are *not independent rotations*, they are the two variables that define the rotation tensor.
- As in the infinitesimal rotations case we only have 5 d.o.f. / node.

##### 4.1.1 Linearization of the equilibrium equations

In Ref. [35] Argyris developed a series expansion for Eqn. (32.a)

$$[{}^{t+\Delta t}R^k] = [I_3] + [\Theta^k] + \frac{1}{2!} [\Theta^k]^2 + \dots \quad (33)$$

Using the above in Eqn. (31) we get

$${}^{t+\Delta t}\underline{\mathbf{V}}_n^k - {}^t\underline{\mathbf{V}}_n^k = \underline{\theta}^k \times {}^t\underline{\mathbf{V}}_n^k + \frac{1}{2} \underline{\theta}^k \times (\underline{\theta}^k \times {}^t\underline{\mathbf{V}}_n^k) + h.o.t. \quad (34.a)$$

where we defined

$$\underline{\theta}^k = \theta_1^k {}^t\underline{\mathbf{V}}_1^k + \theta_2^k {}^t\underline{\mathbf{V}}_2^k \quad (34.b)$$

From Eqns. (34.a) and (34.b) we get

$${}^{t+\Delta t}\underline{\mathbf{V}}_n^k - {}^t\underline{\mathbf{V}}_n^k = (\theta_2^k {}^t\underline{\mathbf{V}}_1^k - \theta_1^k {}^t\underline{\mathbf{V}}_2^k) - \frac{1}{2} [(\theta_1^k)^2 + (\theta_2^k)^2] {}^t\underline{\mathbf{V}}_n^k + h.o.t. \quad (34.c)$$

Hence, for the incremental displacement at a point inside the shell element, in the case of finite rotations instead of Eqn. (2) we get

$$\underline{\mathbf{u}} = h_k \underline{\mathbf{u}}_k + \frac{r_3}{2} h_k {}^t a_k (-\theta_1^k {}^t\underline{\mathbf{V}}_2^k + \theta_2^k {}^t\underline{\mathbf{V}}_1^k) - \frac{r_3}{4} h_k {}^t a_k [(\theta_1^k)^2 + (\theta_2^k)^2] {}^t\underline{\mathbf{V}}_n^k + h.o.t. \quad (35)$$

In the above equation we use the hypothesis that the thickness remains constant during the deformation process ( ${}^{t+\Delta t}a_k = {}^t a_k = \dots = {}^\circ a_k$ ). Hence the formulation that we derive in this Section can only be used for the analysis of cases where the strain components are infinitesimal.

We can also write Eqn. (35) as

$$\underline{\mathbf{u}} = \underline{\mathbf{u}}_I + \underline{\mathbf{u}}_{II} + h.o.t. \quad (36.a)$$

where

$$\underline{\mathbf{u}}_I = h_k \underline{\mathbf{u}}_k + \frac{r_3}{2} h_k {}^t a_k (-\theta_1^k {}^t\underline{\mathbf{V}}_2^k + \theta_2^k {}^t\underline{\mathbf{V}}_1^k) \quad (36.b)$$

$$\underline{\mathbf{u}}_{II} = -\frac{r_3}{4} h_k {}^t a_k [(\theta_1^k)^2 + (\theta_2^k)^2] {}^t\underline{\mathbf{V}}_n^k \quad (36.c)$$

We include in  $\underline{\mathbf{u}}_I$  the terms obtained when considering only infinitesimal rotations and we include in  $\underline{\mathbf{u}}_{II}$  the terms containing  $(\theta_i^k)^2$ .

In the spatial configuration at time  $(t + \Delta t)$  the covariant base vectors of the element natural coordinate system are

$${}^{t+\Delta t}\underline{\tilde{\mathbf{g}}}_i = {}^t\underline{\tilde{\mathbf{g}}}_i + \frac{\partial \underline{\mathbf{u}}}{\partial r_i} \quad (i = 1, 2, 3) \quad (37)$$

Since

$${}^\circ \tilde{\epsilon}_{ij} = \frac{1}{2} \left[ {}^{t+\Delta t}\underline{\tilde{\mathbf{g}}}_i \cdot {}^{t+\Delta t}\underline{\tilde{\mathbf{g}}}_j - {}^\circ \underline{\tilde{\mathbf{g}}}_i \cdot {}^\circ \underline{\tilde{\mathbf{g}}}_j \right] \quad (38.a)$$

using Eqn. (37) we get

$${}^\circ \tilde{\epsilon}_{ij} = {}^\circ \tilde{\epsilon}_{ij} + \underbrace{\frac{1}{2} \left[ {}^t\underline{\tilde{\mathbf{g}}}_i \cdot \frac{\partial \underline{\mathbf{u}}}{\partial r_j} + {}^t\underline{\tilde{\mathbf{g}}}_j \cdot \frac{\partial \underline{\mathbf{u}}}{\partial r_i} + \frac{\partial \underline{\mathbf{u}}}{\partial r_i} \cdot \frac{\partial \underline{\mathbf{u}}}{\partial r_j} \right]}_{{}^\circ \tilde{\epsilon}_{ij} = {}^\circ \tilde{e}_{ij} + {}^\circ \tilde{\eta}_{ij}} \quad (38.b)$$

Using Eqns. (36) and keeping only up to the quadratic terms in generalized incremental displacements, we get

$${}^\circ \tilde{e}_{ij} = \frac{1}{2} \left[ {}^t\underline{\tilde{\mathbf{g}}}_i \cdot \frac{\partial \underline{\mathbf{u}}_I}{\partial r_j} + {}^t\underline{\tilde{\mathbf{g}}}_j \cdot \frac{\partial \underline{\mathbf{u}}_I}{\partial r_i} \right] \quad (39.a)$$

$${}^\circ \tilde{\eta}_{ij} = \frac{1}{2} \left[ {}^t\underline{\tilde{\mathbf{g}}}_i \cdot \frac{\partial \underline{\mathbf{u}}_{II}}{\partial r_j} + {}^t\underline{\tilde{\mathbf{g}}}_j \cdot \frac{\partial \underline{\mathbf{u}}_{II}}{\partial r_i} + \frac{\partial \underline{\mathbf{u}}_I}{\partial r_i} \cdot \frac{\partial \underline{\mathbf{u}}_I}{\partial r_j} \right] \quad (39.b)$$

Note that,

- In elements with no rotational d.o.f. (e.g. 2D and 3D continuum elements) Eqn. (28.c) represents exactly the total strain increments. In our case Eqn. (28.c) represents only an approximation to the strain increments, because in the derivation of Eqn. (39.b) we neglect the terms of order higher than two in generalized displacement increments.
- Equations (39) contain all the terms up to the second order in generalized displacement increments. This guarantees a *complete quadratic form of the incremental energy*, leading therefore to a *consistent tangent stiffness matrix*.

## 4.2 Nonlinear formulation for the MITC shell elements

For the standard A-I-Z shell element, the incremental displacements are calculated using Eqn. (35) and the incremental strains are directly calculated using Eqns. (39).

For the MITC elements the incremental displacements are calculated in the same way, but the incremental strains are interpolated using the interpolation formulae that we presented in Section 3.

### 4.2.1 MITC4 shell element

- The “in-layer” strain incremental components  $(\circ\tilde{e}_{11}, \circ\tilde{e}_{22}, \circ\tilde{e}_{12})$  and  $(\circ\tilde{\eta}_{11}, \circ\tilde{\eta}_{22}, \circ\tilde{\eta}_{12})$  are directly calculated from the incremental displacements interpolation.
- The transverse shear strain incremental components  $(\circ\tilde{e}_{13}, \circ\tilde{e}_{23})$  and  $(\circ\tilde{\eta}_{13}, \circ\tilde{\eta}_{23})$  are interpolated using Eqns. (11).

In order to illustrate on the behavior of the MITC4 shell element in nonlinear analyses we present in Figures 17 to 19 some selected examples.

### 4.2.2 MITC8 shell element

- The “in-layer” incremental strain components  $(\circ\tilde{e}_{11}, \circ\tilde{e}_{22}, \circ\tilde{e}_{12})$  and  $(\circ\tilde{\eta}_{11}, \circ\tilde{\eta}_{22}, \circ\tilde{\eta}_{12})$  are interpolated using Eqns. (16).
- The incremental transverse shear strain components  $(\circ\tilde{e}_{13}, \circ\tilde{e}_{23})$  and  $(\circ\tilde{\eta}_{13}, \circ\tilde{\eta}_{23})$  are interpolated using Eqns. (17) to (19).

In order to illustrate on the behavior of the MITC8 shell element in nonlinear analyses we present in Figures 20 and 21 some selected examples.

## 5. FINITE STRAIN ELASTO-PLASTIC FORMULATION

The modelling of some industrial processes like sheet metal forming and the simulation of impact problems in metallic shell structures require the use of a finite strain elasto-plastic shell analysis capability.

In our Ref. [23] we developed a new formulation for the MITC4 shell element for finite strain elasto-plastic analysis.

The new MITC4 formulation is based on:

- The interpolations presented in Section 3 for the MITC4 shell element.
- Lee’s multiplicative decomposition of the deformation gradient [36,37].
- The hyperelastic expression of the Von Mises flow theory developed using the principle of maximum plastic dissipation [38-42] (associated flow rule [43]).

Following our previous developments for 2D analysis [44] in Ref. [23] we presented a *Total Lagrangian-Hencky formulation for the MITC4 shell element* (MITC4-TLH) using a

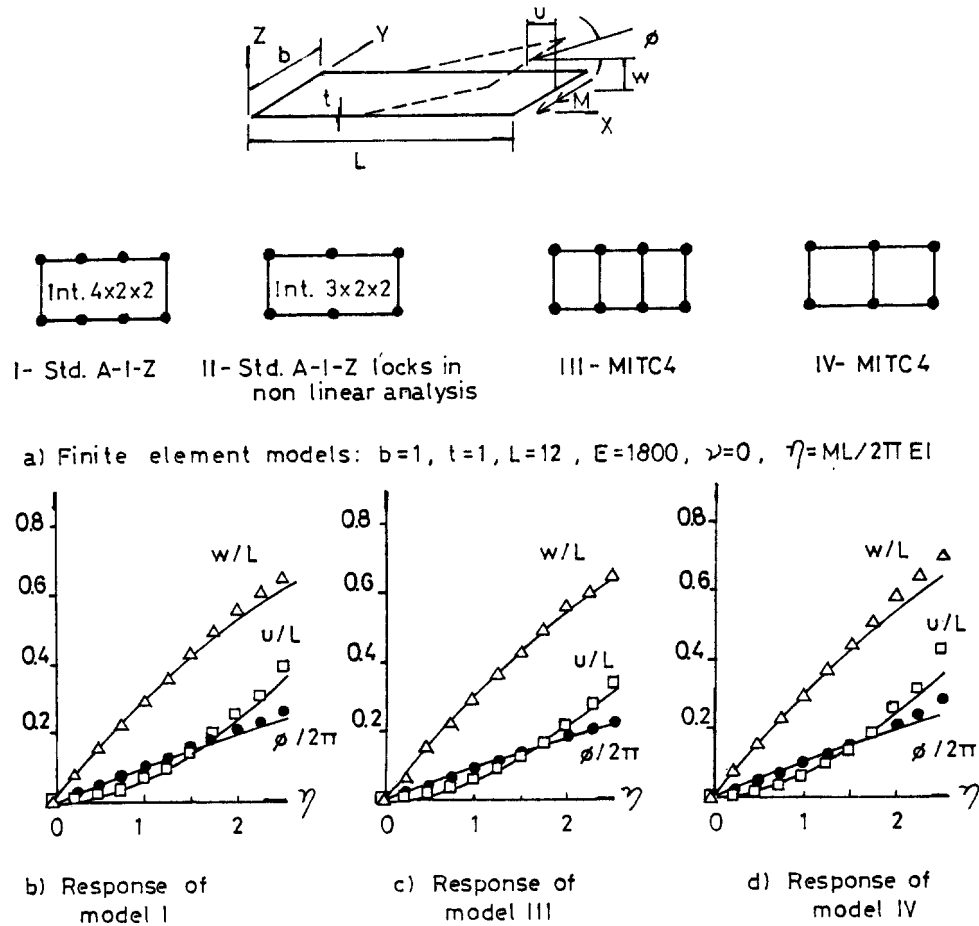


**Figure 17.** Large deflection analysis of a cantilever using MITC4 elements. (The lines indicate the analytical results and the symbols  $\Delta$ ,  $\diamond$  and  $\bullet$  the numerical results)

hyperelastic constitutive equation in terms of Hencky’s logarithmic strain tensor and its work conjugate stress tensor [45,46].

The kinematic description of the MITC4-TLH shell element incorporates 5 d.o.f. per node (see Section 3) and also a *thickness stretching* interpolation with one thickness stretching d.o.f. per Gauss point.

We use a general 3D constitutive relation and condense the thickness stretching d.o.f. at the elements level by imposing at each Gauss point Love’s fourth postulate [47]:  ${}^t\sigma_{nn} = 0$ ; where  ${}^t\sigma_{nn}$  is the Cauchy stress component in the shell normal direction  ${}^t\underline{n}$  in the spatial configuration.

It is important to mention that other Authors have previously developed finite strain shell elements. Among them we can reference:

- Rodal and Witmer [48] in 1979 developed a shell element for elasto-plastic analysis that *a posteriori* of the displacement calculations updates the shell thickness. The thickness update is performed for materials following a Von Mises associated plasticity flow rule neglecting the elastic volumetric strain.
- Hughes and Carnoy [49] in 1983 developed a finite strain shell element for the Mooney-Rivlin material. Their element uses plane stress constitutive relations for the laminae

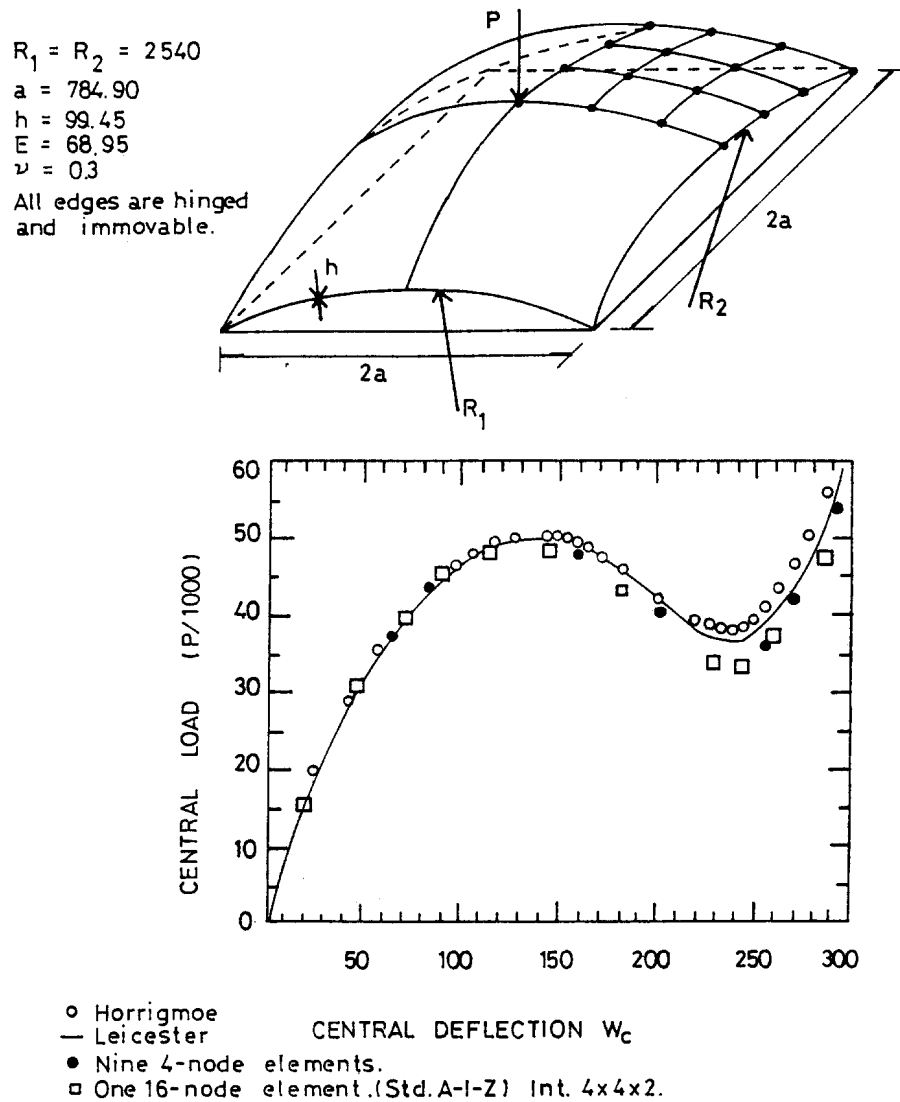


Figure 18. Nonlinear spherical shell (MITC4)

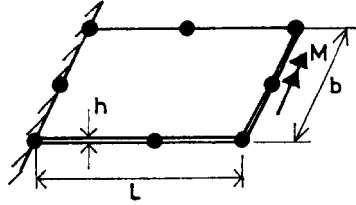
and also updates the shell thickness *a posteriori* of the displacements calculation in a staggered iterative calculation.

- Simo and co-workers [50-54] in the period 1988-1992 developed a shell element formulation that includes the possibility of finite elasto-plastic shell analysis using a *fully consistent extensible thickness* approach. Since this shell element works with stress resultants an *Ilyushin type plasticity model* is used.

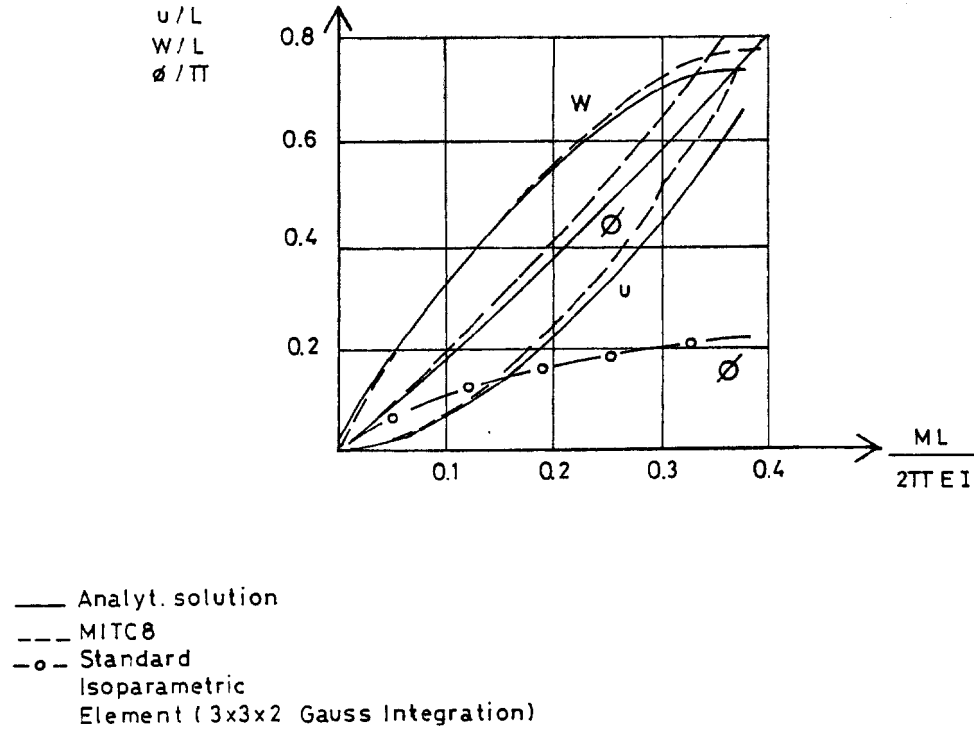
Comparing the MITC4-TLH formulation with the above ones we can mention that as compared with the two first ones the MITC4-TLH formulation introduces the “in-layer” plane stress condition consistently, and as compared with Simo’s et al. formulation we do



$L = 12$   
 $b = 1$   
 $h = 1$   
 $E = 1800$   
 $\nu = 0$



a) Problem and mesh.



b) Solution.

Figure 20. Large deflection analysis of cantilever using MITC8 elements

$$\begin{aligned}
 &= h_k(r_1, r_2) {}^t \underline{\mathbf{u}}_k + \frac{1}{2} h_k(r_1, r_2) \left[ \int_0^{r_3} {}^t \lambda(r_1, r_2, s) ds \right] {}^\circ a_k {}^t \underline{\mathbf{V}}_n^k \\
 &\quad - \frac{r_3}{2} h_k(r_1, r_2) {}^\circ a_k {}^\circ \underline{\mathbf{V}}_n^k
 \end{aligned} \tag{40}$$

where  ${}^t \lambda(r_i)$  is the thickness stretching at the point with natural (convected) coordinates  $(r_i)$ .

During the iterative solving processes it is important to avoid negative numerical values of  ${}^t \lambda$  (non-physical values), therefore we use the variable [54]

$${}^t \xi(r_i) = \ln {}^t \lambda(r_i) \tag{41.a}$$

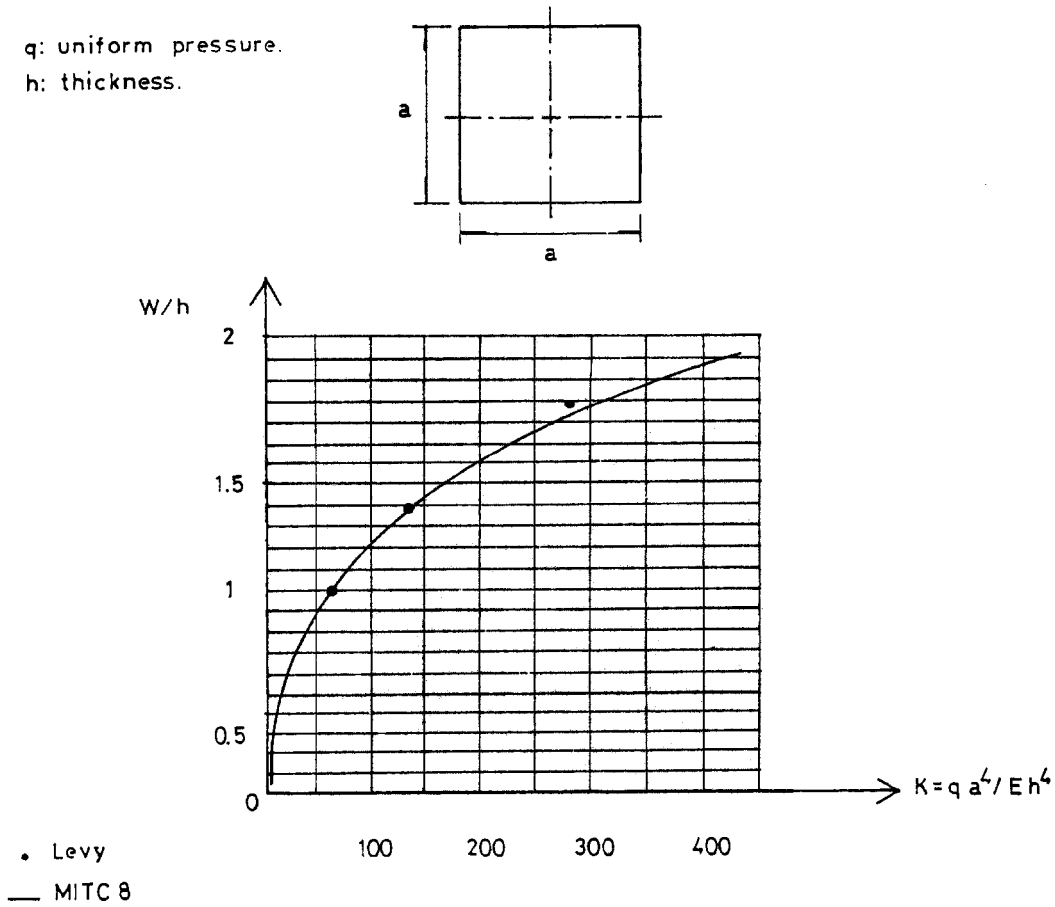


**Figure 21.** Nonlinear analysis of a linear elastic plate under uniform pressure using the MITC8 element. (Four elements were used to model one quarter of the plate)

In the finite element discretization, we use the following interpolation

$${}^t\xi(r_i) = h_j^G(r_i) {}^t\xi_j \quad (41.b)$$

where  $h_j^G$  is a Lagrangian polynomial that takes a unit value at the  $j$ -th Gauss point and a zero value at all the other integration points. Also  ${}^t\xi_j$  is the value of  ${}^t\xi(r_i)$  at the  $j$ -th Gauss point.

Using Eqns. (41) in Eqn. (40) we get

$${}^t\mathbf{u} = h_k {}^t\mathbf{u}_k + \frac{1}{2} h_k \left[ \int_0^{r_3} \exp(h_j^G {}^t\xi_j) ds \right] {}^o a_k {}^t\mathbf{V}_n^k - \frac{r_3}{2} h_k {}^o a_k {}^o\mathbf{V}_n^k \quad (42)$$

Since we eliminate the  ${}^t\xi_j$  d.o.f. at the element level, the MITC4-TLH shell element like all the shell elements of the A-I-Z family, presents 5 d.o.f. / node.

## 5.2 Strain interpolations

From Eqn. (40) we can calculate the deformation gradient tensor [27-28] derived from the *displacement interpolation*:  ${}^t\underline{\underline{\mathbf{F}}}^{DI}$ , at any point inside the element.

Using a right polar decomposition [27,28]

$${}^t\underline{\underline{\mathbf{F}}}^{DI} = {}^t\underline{\underline{\mathbf{R}}}^{DI} \cdot {}^t\underline{\underline{\mathbf{U}}}^{DI} \quad (43.a)$$

The Hencky strain tensor derived from the displacement interpolation is

$${}^t\underline{\underline{\mathbf{H}}}^{DI} = {}^t\tilde{H}_{ij}^{DI} \circ \underline{\underline{\mathbf{g}}}^i \circ \underline{\underline{\mathbf{g}}}^j = \ln {}^t\underline{\underline{\mathbf{U}}}^{DI} \quad (43.b)$$

To avoid shear locking we interpolate the covariant strain components of the Hencky strain tensor using the same interpolations that we used in Section 3:

- The “in-layer” strain components are directly

$${}^t\tilde{H}_{ij} = {}^t\tilde{H}_{ij}^{DI} \quad ; \quad i, j = 1, 2 \quad (44)$$

- The transverse shear strains are interpolated with the formulae schematized previously in Figure 5

$${}^t\tilde{H}_{13} = \frac{1}{2} (1 + r_2) {}^t\tilde{H}_{13}|_A^{DI} + \frac{1}{2} (1 - r_2) {}^t\tilde{H}_{13}|_C^{DI} \quad (45.a)$$

$${}^t\tilde{H}_{23} = \frac{1}{2} (1 + r_1) {}^t\tilde{H}_{23}|_D^{DI} + \frac{1}{2} (1 - r_1) {}^t\tilde{H}_{23}|_B^{DI} \quad (45.b)$$

Where the  ${}^t\tilde{H}_{ij}|_P^{DI}$  are the covariant strain components of the Hencky strain tensor, calculated at the sampling point  $P$ , from the displacement interpolation.

Using Eqns. (44) and (45) we can write

$${}^t\underline{\underline{\mathbf{H}}} = {}^t\tilde{H}_{ij} \circ \underline{\underline{\mathbf{g}}}^i \circ \underline{\underline{\mathbf{g}}}^j \quad (46)$$

The rotation, right stretch and deformation gradient tensors *consistent* with the above interpolations are

$${}^t\underline{\underline{\mathbf{R}}} = {}^t\underline{\underline{\mathbf{R}}}^{DI} \quad (47.a)$$

$${}^t\underline{\underline{\mathbf{U}}} = \exp({}^t\underline{\underline{\mathbf{H}}}) \quad (47.b)$$

$${}^t\underline{\underline{\mathbf{F}}} = {}^t\underline{\underline{\mathbf{R}}} \cdot {}^t\underline{\underline{\mathbf{U}}} = {}^t\underline{\underline{\mathbf{R}}}^{DI} \cdot \exp({}^t\underline{\underline{\mathbf{H}}}) \quad (47.c)$$

## 5.3 The total Lagrangian-Hencky formulation

We can define the pull-back of the Kirchhoff stress tensor under the rotation  ${}^t\underline{\underline{\mathbf{R}}}$  [55,26]

$${}^t\Gamma^{IJ} = [{}^tR^*({}^t\tau^{ij})]^{IJ} \quad (48.a)$$

$${}^t\Gamma^{IJ} = ({}^tR^T)^I_i {}^t\tau^{ij} ({}^tR^T)^J_j \quad (48.b)$$

It is important to realize that  ${}^t\underline{\underline{\mathbf{T}}}$  is a tensor obtained via a rotation of  ${}^t\underline{\underline{\mathbf{T}}}$ .

It has been shown by Atluri [46] that for *isotropic materials* the stress work rate per unit volume of the reference configuration is

$${}^t\dot{W}_\circ = {}^t\underline{\underline{\mathbf{T}}} : \frac{d}{dt}({}^t\underline{\underline{\mathbf{H}}}) \quad (49)$$

In an isotropic material  ${}^t\underline{\underline{\sigma}}$  and  ${}^t\underline{\underline{\mathbf{V}}}$  (left stretch tensor) are coaxial, and since [26]

$${}^tH_{IJ} = \ln [{}^tR^*({}^tV_{ij})]_{IJ} \quad (50)$$

it is obvious that in an isotropic material  ${}^t\underline{\underline{\mathbf{T}}}$  and  ${}^t\underline{\underline{\mathbf{H}}}$  are also coaxial.

### 5.3.1 Kinematics of finite elasto-plastic deformations

For a solid continuum body  $\mathcal{B}$  undergoing an elasto-plastic deformation process, we present in Figure 22 a scheme of Lee's multiplicative decomposition of the deformation gradient [36,37]. The intermediate (unstressed) configuration does not need to be an actual configuration of the body  $\mathcal{B}$  because it does not need to be a smooth homeomorphism of  $\mathcal{B}$  onto a 3D-Euclidean space [27] and in general it will not be an actual configuration [36,37].

For the multiplicative decomposition

$${}^t\underline{\underline{\mathbf{F}}} = {}^t\underline{\underline{\mathbf{F}}}_e \cdot {}^t\underline{\underline{\mathbf{F}}}_p \quad (51)$$

It is immediate to show that in the spatial configuration the velocity gradient is given by [23]

$${}^t\underline{\underline{\mathbf{l}}} = {}^t\underline{\underline{\dot{\mathbf{F}}}}_e \cdot {}^t\underline{\underline{\mathbf{F}}}_e^{-1} + {}^tF_{e*}({}^t\underline{\underline{\mathbf{l}}}_p) \quad (52.a)$$

In the above we used

$${}^t\underline{\underline{\mathbf{l}}}_p = {}^t\underline{\underline{\dot{\mathbf{F}}}}_p \cdot {}^t\underline{\underline{\mathbf{F}}}_p^{-1} \quad (52.b)$$

and also, by similarity with Eqns. (48)

$${}^tF_{e*}({}^t\underline{\underline{\mathbf{l}}}_p) = {}^t\underline{\underline{\mathbf{F}}}_e \cdot {}^t\underline{\underline{\mathbf{l}}}_p \cdot {}^t\underline{\underline{\mathbf{F}}}_e^{-1} \quad (52.c)$$

We can make an additive decomposition of  ${}^t\underline{\underline{\mathbf{l}}}_p$  into a symmetric tensor ( ${}^t\underline{\underline{\mathbf{d}}}$ ) and a skew-symmetric one ( ${}^t\underline{\underline{\omega}}$ ) [36,37].

For a material with *isotropic elastic properties* we can impose  ${}^t\underline{\underline{\omega}} = \underline{\underline{\mathbf{0}}}$ .

### 5.3.2 Stresses in finite strain elasto-plastic problems

By doing the polar decomposition of  ${}^t\underline{\underline{\mathbf{F}}}_e$  and  ${}^t\underline{\underline{\mathbf{F}}}_p$  we get

$${}^t\underline{\underline{\mathbf{F}}}_e = {}^t\underline{\underline{\mathbf{R}}}_e \cdot {}^t\underline{\underline{\mathbf{U}}}_e = {}^t\underline{\underline{\mathbf{V}}}_e \cdot {}^t\underline{\underline{\mathbf{R}}}_e \quad (53.a)$$

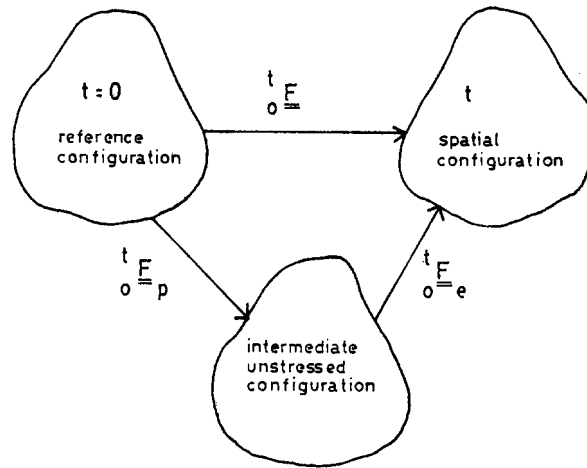
$${}^t\underline{\underline{\mathbf{F}}}_p = {}^t\underline{\underline{\mathbf{R}}}_p \cdot {}^t\underline{\underline{\mathbf{U}}}_p = {}^t\underline{\underline{\mathbf{V}}}_p \cdot {}^t\underline{\underline{\mathbf{R}}}_p \quad (53.b)$$

and we can define the *elastic Hencky strain tensor*

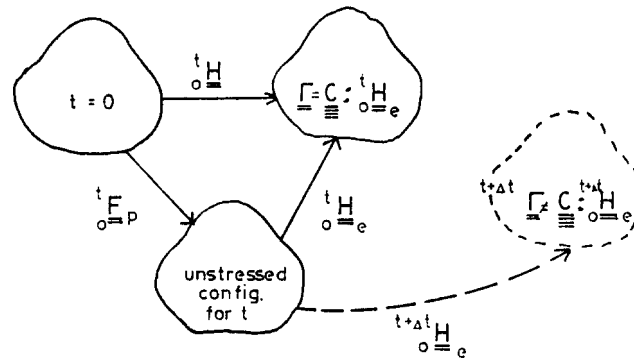
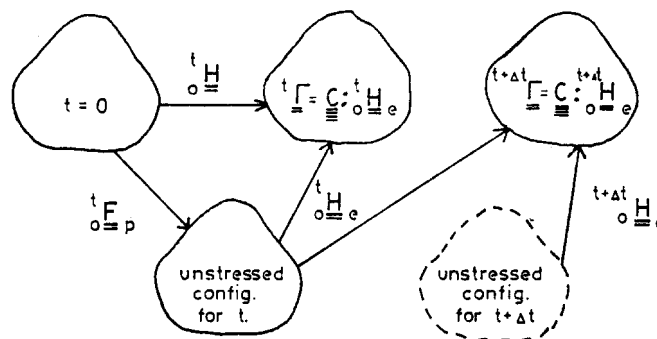
$${}^t\underline{\underline{\mathbf{H}}}_e = \ln \left( {}^t\underline{\underline{\mathbf{U}}}_e \right) \quad (54)$$

Considering that stresses are developed when the intermediate configuration evolves into the spatial configuration, following Eqns. (48) and by means of the notation abuse used in Eqn. (52.c) we define

$${}^t\underline{\underline{\mathbf{T}}} = {}^tR_e^*({}^t\underline{\underline{\mathbf{T}}}) \quad (55)$$



a) Lee's multiplicative decomposition.

b.1) Determination of the configuration at  $t+\Delta t$ 

b.2) Updating of the intermediate configuration.

b) Incremental formulation.

Figure 22. Finite strain elasto-plastic analysis

### 5.3.3 The yield criterion

Following the work by Lee [36,37] we formulate the yield criterion in the spatial configuration in terms of Kirchhoff stresses.

Since we are interested in the behaviour of metallic shells we use the Von Mises ( $J_2$ ) yield criterion. Considering the case of isotropic hardening we get, for the yield criterion

$${}^t\phi = \left[ \frac{3}{2} {}^t\underline{\underline{\tau}}_D : {}^t\underline{\underline{\tau}}_D \right]^{\frac{1}{2}} - {}^t\sigma_y = 0 \quad (56)$$

In the above,  ${}^t\underline{\underline{\tau}}_D$  is the deviatoric Kirchhoff stress tensor. It is important to notice that the tensor defined by

$${}^t\underline{\underline{\Gamma}}_D = {}^t\circ R_e^*({}^t\underline{\underline{\tau}}_D) \quad (57)$$

is also deviatoric (traceless). By doing an  ${}^t\circ R_e$ -pull-back an Eqn. (56) we get for the yield criterion

$${}^t\phi = \left[ \frac{3}{2} {}^t\underline{\underline{\Gamma}}_D : {}^t\underline{\underline{\Gamma}}_D \right]^{\frac{1}{2}} - {}^t\sigma_y = 0 \quad (58)$$

For the yield stress,  ${}^t\sigma_y$ , we define the following evolution equation (hardening)

$${}^t\dot{\sigma}_y = h {}^t\dot{\bar{e}}_p \quad (59)$$

where  $h = h({}^t\bar{e}_p)$  is the hardening modulus and  ${}^t\bar{e}_p$  is the equivalent plastic strain, to be defined in what follows.

### 5.3.4 Energy dissipation

We now introduce the *free energy function* defined in the spatial configuration, per unit volume of the reference configuration:  ${}^t\Psi$ .

For a pure mechanical problem, the Clausius-Duhem inequality (*principle of dissipation*) [27] takes the form

$${}^t\underline{\underline{\tau}} : {}^t\underline{\underline{\mathbf{d}}} - {}^t\dot{\Psi} \geq 0 \quad (60.a)$$

$${}^t\underline{\underline{\mathbf{d}}} = \text{sym}({}^t\underline{\underline{\mathbf{l}}}) \quad (60.b)$$

In the above

$${}^t\Psi = {}^t\Psi({}^t\circ\underline{\underline{\mathbf{H}}}_e, {}^t\bar{e}_p) \quad (60.c)$$

After Simo [41] we use the following uncoupled expression for the free energy

$${}^t\Psi = {}^t\Psi_e({}^t\circ\underline{\underline{\mathbf{H}}}_e) + {}^t\Psi_p({}^t\bar{e}_p) \quad (60.d)$$

Using the notation

$${}^t\underline{\underline{\mathbf{l}}}_e = {}^t\circ\underline{\underline{\mathbf{F}}}_e \cdot {}^t\circ\underline{\underline{\mathbf{F}}}_e^{-1} = {}^t\underline{\underline{\mathbf{d}}}_e + {}^t\underline{\underline{\omega}}_e \quad (61.a)$$

$${}^t\underline{\underline{\mathbf{l}}}_p = {}^t\circ F_{e^*}({}^t\underline{\underline{\mathbf{l}}}_p) = {}^t\underline{\underline{\mathbf{d}}}_p + {}^t\underline{\underline{\omega}}_p \quad (61.b)$$

we can write

$${}^t_{\underline{\underline{\Gamma}}}: {}^t_{\underline{\underline{\mathbf{d}}}} = {}^t_{\underline{\underline{\Gamma}}}: \left( {}^t_{\underline{\underline{\mathbf{d}}}_e} + {}^t_{\underline{\underline{\mathbf{d}}}_p} \right) \quad (62.a)$$

For an elastically isotropic material

$${}^t_{\underline{\underline{\Gamma}}}: {}^t_{\underline{\underline{\mathbf{d}}}_e} = {}^t_{\underline{\underline{\Gamma}}}: \frac{d}{dt} \left( {}^t_{\circ} \underline{\underline{\mathbf{H}}}_e \right) \quad (62.b)$$

and we can show, after some algebra, that

$${}^t_{\underline{\underline{\Gamma}}}: {}^t_{\underline{\underline{\mathbf{d}}}_p} = \left[ {}^t_{\circ} \underline{\underline{\mathbf{F}}}^T \cdot {}^t_{\underline{\underline{\Gamma}}} \cdot {}^t_{\circ} \underline{\underline{\mathbf{F}}}^{-T} \right] : {}^t_{\underline{\underline{\mathbf{I}}}_p} \quad (62.c)$$

Using the above results we can write the Clausius-Duhem inequality as

$$\left[ {}^t_{\underline{\underline{\Gamma}}} - \frac{\partial {}^t \Psi_e}{\partial {}^t_{\circ} \underline{\underline{\mathbf{H}}}_e} \right] : \frac{d}{dt} \left( {}^t_{\circ} \underline{\underline{\mathbf{H}}}_e \right) + \left[ {}^t_{\circ} \underline{\underline{\mathbf{F}}}^T \cdot {}^t_{\underline{\underline{\Gamma}}} \cdot {}^t_{\circ} \underline{\underline{\mathbf{F}}}^{-T} \right] : {}^t_{\underline{\underline{\mathbf{I}}}_p} - {}^t \dot{\Psi}_p \geq 0 \quad (63)$$

In the case of a pure elastic deformation the above equation leads to

$${}^t_{\underline{\underline{\Gamma}}} = \frac{\partial {}^t \Psi_e}{\partial {}^t_{\circ} \underline{\underline{\mathbf{H}}}_e} \quad (64)$$

Hence

$${}^t D = \left[ {}^t_{\circ} \underline{\underline{\mathbf{F}}}^T \cdot {}^t_{\underline{\underline{\Gamma}}} \cdot {}^t_{\circ} \underline{\underline{\mathbf{F}}}^{-T} \right] : {}^t_{\underline{\underline{\mathbf{I}}}_p} - {}^t \dot{\Psi}_p \geq 0 \quad (65.a)$$

where  ${}^t D$  is called *dissipation* [41].

For elastically isotropic materials we can re-write Eqn. (65.a) as

$${}^t D = {}^t_{\underline{\underline{\Gamma}}}: {}^t_{\underline{\underline{\mathbf{d}}}_p} - {}^t \dot{\Psi}_p \geq 0 \quad (65.b)$$

Using the *Principle of Maximum Plastic Dissipation* (associated flow rule) [56] we have to

- maximize  ${}^t D$
- under the constraint  ${}^t \phi \leq 0$ .

The Khun-Tucker conditions [57] for the above constraint maximization problem lead to

$${}^t_{\underline{\underline{\mathbf{d}}}_p} = {}^t \lambda \frac{\partial {}^t \phi}{\partial {}^t_{\underline{\underline{\mathbf{d}}}_p}} \quad (66.a)$$

where  ${}^t \lambda$  is a positive parameter. In addition to the above we get

$${}^t \lambda \quad {}^t \phi = 0 \quad (66.b)$$

From the above

$${}^t \lambda = 0 \quad \text{if} \quad {}^t \phi < 0 \quad (66.c)$$

$${}^t \lambda > 0 \quad \text{if} \quad {}^t \phi = 0 \quad (66.d)$$

Please notice that Eqn. (66.a) is the well known *normality-rule* [43,56] of associated plasticity.

We define the *equivalent plastic strain rate* as [43]

$${}^t\dot{\underline{\underline{c}}}_p = \left[ \frac{2}{3} {}^t\underline{\underline{d}} : {}^t\underline{\underline{d}}_p \right]^{\frac{1}{2}} \quad (67)$$

and from Eqn. (66.a)

$${}^t\lambda = {}^t\dot{\underline{\underline{c}}}_p \left[ \frac{3}{2 \left( \frac{\partial {}^t\phi}{\partial \underline{\underline{\Gamma}}} : \frac{\partial {}^t\phi}{\partial \underline{\underline{\Gamma}}} \right)} \right]^{\frac{1}{2}} \quad (68)$$

Using Eqn. (58) in the above ones we get

$${}^t\underline{\underline{d}}_p = \frac{3}{2} {}^t\dot{\underline{\underline{c}}}_p \frac{{}^t\underline{\underline{\Gamma}}_D}{\left[ \frac{3}{2} {}^t\underline{\underline{\Gamma}}_D : {}^t\underline{\underline{\Gamma}}_D \right]^{\frac{1}{2}}} \quad (69)$$

#### 5.4 Calculation of stresses, plastic variables and thickness stretchings

Concentrating on the case of an elastic behavior linear and isotropic we write

$${}^t\Psi_e = \frac{1}{2} {}^t\underline{\underline{\mathbf{H}}}_e : \underline{\underline{\mathbf{C}}} : {}^t\underline{\underline{\mathbf{H}}}_e \quad (70)$$

where  $\underline{\underline{\mathbf{C}}}$  is an isotropic and constant fourth order tensor (Hooke's law).

The condition of zero stresses through the thickness (spatial configuration) leads to

$${}^t\sigma_{nn} = {}^t\tau_{nn} = [{}^tR_e({}^t\underline{\underline{\tau}})]_{NN} = 0 \quad (71)$$

where  ${}^t\underline{\underline{\mathbf{n}}} = {}^t\underline{\underline{\mathbf{R}}}_e \cdot \underline{\underline{\mathbf{N}}}$ .

In the space of the  $R_e$ -pull-back we do not know *a priori* the N-direction for which  ${}^t\Gamma_{NN} = 0$ . Hence we cannot include in  $\underline{\underline{\mathbf{C}}}$  the “in-layer” plane stress hypothesis. Therefore we use the standard 3D constitutive tensor, and the plane stress hypothesis is enforced via the iterative algorithm that we present in the following Section.

##### 5.4.1 Iterative algorithm for calculating thickness stretchings

The incremental step from the  $t$ -configuration to the  $(t + \Delta t)$ -configuration is solved with an iterative scheme, and for each iteration

- Trial values are proposed, in some way, for the mid-surface nodes position  $({}^{t+\Delta t}\underline{\underline{\mathbf{x}}}^k)$  and for the director vectors  $({}^{t+\Delta t}\underline{\underline{\mathbf{V}}}_n^k)$ .
- Stresses, plastic variables and thickness stretchings are determined for the trial  $(t + \Delta t)$ -configuration.

For each element:

- we start from the data corresponding to the previous equilibrium configuration  $\left\{ {}^t\underline{\underline{\mathbf{F}}}_p ; {}^t\sigma_y ; {}^t\xi \right\}$  at each Gauss point.
- we calculate those quantities at the trial  $(t + \Delta t)$ -configuration.

At every Gauss point in the  $(t + \Delta t)$ -configuration we need to satisfy the following requirements:

$$\begin{aligned} {}^{t+\Delta t}\tau_{nn}|_k \left( {}^{t+\Delta t}\underline{\mathbf{x}}_q ; {}^{t+\Delta t}\underline{\mathbf{V}}_n^q ; {}^{t+\Delta t}\underline{\mathbf{e}}_p^q ; {}^{t+\Delta t}\underline{\xi}_q \right) &= 0 \\ {}^{t+\Delta t}\phi|_k \left( {}^{t+\Delta t}\underline{\mathbf{x}}_q ; {}^{t+\Delta t}\underline{\mathbf{V}}_n^q ; {}^{t+\Delta t}\underline{\mathbf{e}}_p^q ; {}^{t+\Delta t}\underline{\xi}_q \right) &= 0 \end{aligned} \quad k, q = 1, \dots, NG \quad (72)$$

Having  $NG$  Gauss points per element, Eqns. (72) represent a system of  $(2 * NG)$  nonlinear equations, with  $({}^{t+\Delta t}\underline{\mathbf{e}}_p^q$  and  ${}^{t+\Delta t}\underline{\xi}^q ; q = 1, \dots, NG)$  as unknowns.

It is important to notice that Eqns. (72) are *not decoupled* as in the case of the standard radial return-algorithm.

To solve the nonlinear system given by Eqns. (72) we use, at the element level, the iterative algorithm shown in Box I.

#### 5.4.2 Radial return algorithm

We use general 3D radial return algorithm.

For each Gauss point the data is

$$\begin{aligned} &- {}^{\circ}{}^{t+\Delta t}\underline{\mathbf{F}}({}^{t+\Delta t}\underline{\mathbf{x}}_k ; {}^{t+\Delta t}\underline{\mathbf{V}}_n^k ; {}^{t+\Delta t}\underline{\xi}) \\ &- {}^{\circ}{}^{t+\Delta t}\underline{\mathbf{H}} ; {}^{\circ}{}^{t+\Delta t}\underline{\mathbf{U}} ; {}^{\circ}{}^{t+\Delta t}\underline{\mathbf{C}} \\ &- {}^{\circ}{}^{t+\Delta t}\underline{\mathbf{F}}_p \text{ and } {}^{t+\Delta t}\sigma_y \end{aligned}$$

and we search for:  ${}^{\circ}{}^{t+\Delta t}\underline{\mathbf{F}}_p ; {}^{t+\Delta t}\sigma_y$  and  ${}^{t+\Delta t}\underline{\mathbf{I}}$ .

Therefore, at each Gauss point we go through the calculation procedure shown in Box II.

The equations used in the radial return algorithm were derived in our Refs. [23,44], following the derivations in Ref. [58].

The reader should realize at this point that:

- The total strains are interpolated from the sampling points.
- The stresses and plastic variables are only calculated at the integration points, using the presented radial return algorithm.

#### 5.5 The incremental formulation

The equilibrium configuration at time (load level)  $t + \Delta t$  has to fulfil the Principle of Virtual Work

$$\int_{t+\Delta t_V} {}^{t+\Delta t}\sigma^{ij} \delta e_{ij} \, dv = {}^{t+\Delta t}\mathfrak{R} \quad (73.a)$$

where

$t + \Delta t_V$  : volume of the spatial configuration at  $t + \Delta t$ .

${}^{t+\Delta t}\sigma^{ij}$  : contravariant components of the Cauchy stress tensor in the  $(t + \Delta t)$ -configuration.

$e_{ij} = \frac{1}{2} (u_i|_j + u_j|_i)$  where  $u_i$  are incremental displacements measured from the  $(t + \Delta t)$ -configuration.

${}^{t+\Delta t}\mathfrak{R}$  : virtual work of the external loads acting on the  $(t + \Delta t)$ -configuration.

• Iterative algorithm at the elements level

$${}^{t+\Delta t}\underline{\underline{\mathbf{e}}}_p = \{ {}^{t+\Delta t}\underline{\underline{\mathbf{e}}}_p^q \} \quad ; \quad {}^{t+\Delta t}\underline{\underline{\xi}} = \{ {}^{t+\Delta t}\underline{\underline{\xi}}_q \}$$

1

$$i = 0 \\ {}^{t+\Delta t}\underline{\underline{\xi}}^{(i)} = \underline{\underline{\xi}}$$

2

- . Calculate at each Gauss point  ${}_{\circ}^{t+\Delta t}\underline{\underline{\mathbf{H}}}^{(i)}$  using Eqns. (43) to (46).
- . Calculate at each Gauss point  ${}_{\circ}^{t+\Delta t}\underline{\underline{\mathbf{U}}}^{(i)}$  using Eq. (47.b).
- . Calculate at each Gauss point  ${}_{\circ}^{t+\Delta t}\underline{\underline{\mathbf{C}}}^{(i)} = \left( {}_{\circ}^{t+\Delta t}\underline{\underline{\mathbf{U}}}^{(i)} \right)^T \cdot {}_{\circ}^{t+\Delta t}\underline{\underline{\mathbf{U}}}^{(i)}$ .

3

Using the radial return algorithm (Section 5.4.2.) calculate at each Gauss point,

$${}^{t+\Delta t}\underline{\underline{\mathbf{T}}}^{(i)} \quad \text{and} \quad {}_{\circ}^{t+\Delta t}\underline{\underline{\mathbf{R}}}_e^{(i)}$$

4

Calculate at each Gauss point (k),

$${}^{t+\Delta t}\tau_{nn}^{(i)}|_k = {}^{t+\Delta t}\underline{\underline{\mathbf{V}}}_n^k \cdot \left[ {}_{\circ}^{t+\Delta t}\underline{\underline{\mathbf{R}}}_{e*}^{(i)}({}^{t+\Delta t}\underline{\underline{\mathbf{T}}}^{(i)}) \right] \cdot {}^{t+\Delta t}\underline{\underline{\mathbf{V}}}_n^k$$

5

Determine:  $\tau_{nn}^{max} = \max(\text{abs}({}^{t+\Delta t}\tau_{nn}^{(i)}|_k)) \quad ; \quad k = 1, 2, \dots, NG$

6

IF (  $\tau^{max} \leq E * \text{TolNN}$  ) THEN  
the inner loop has converged

ELSE

go to 7

E: Young's modulus

TolNN =  $1.E - 8$  in our numerical implementation

7

$i = i + 1$

At each Gauss point (k):

$${}^{t+\Delta t}\tau_{nn}^{(i-1)}|_k + \sum_{q=1}^{NG} \left\{ \frac{\partial \tau_{nn}}{\partial \xi_q} \Big|_k^{(i-1)} + \left[ \frac{\partial \tau_{nn}}{\partial \bar{\mathbf{e}}_p} \frac{\partial \bar{\mathbf{e}}_p}{\partial \xi_q} \right]_k^{(i-1)} \right\} \\ \left[ {}^{t+\Delta t}\underline{\underline{\xi}}_q^{(i)} - {}^{t+\Delta t}\underline{\underline{\xi}}_q^{(i-1)} \right]_k = 0$$

The derivatives in the above equation are calculated in Appendix I.

The above NG linear equations provide  ${}^{t+\Delta t}\underline{\underline{\xi}}^{(i)}$

8

Improve the value of  ${}^{t+\Delta t}\underline{\underline{\xi}}^{(i)}$  using a line search procedure along the direction:

$${}^{t+\Delta t}\underline{\underline{\xi}}^{(i)} - {}^{t+\Delta t}\underline{\underline{\xi}}^{(i-1)}$$

9

GO TO step 2

**Box I**

• Radial return algorithm at each Gauss point

*Elastic predictor*

$$\hat{\underline{\underline{\mathbf{F}}}}_p = {}^t \underline{\underline{\mathbf{F}}}_p \quad (\text{trial value})$$

$$\hat{\sigma}_y = {}^t \sigma_y \quad (\text{trial value})$$

$$\hat{\underline{\underline{\mathbf{C}}}}_e = \left( \hat{\underline{\underline{\mathbf{F}}}}_p \right)^{-T} \cdot {}^{t+\Delta t} \underline{\underline{\mathbf{C}}}_e \cdot \left( \hat{\underline{\underline{\mathbf{F}}}}_p \right)^{-1}$$

$$\hat{\underline{\underline{\mathbf{H}}}}_e = \ln \left[ \left( \hat{\underline{\underline{\mathbf{C}}}}_e \right)^{-\frac{1}{2}} \right]$$

$$\hat{\underline{\underline{\mathbf{T}}}} = \underline{\underline{\mathbf{C}}} : \hat{\underline{\underline{\mathbf{H}}}}_e$$

$$\hat{\phi} = \left[ \frac{3}{2} \hat{\underline{\underline{\mathbf{T}}}}_D : \hat{\underline{\underline{\mathbf{T}}}}_D \right]^{\frac{1}{2}} - \hat{\sigma}_y$$

IF (  $\hat{\phi} \leq 0$  ) THEN

$${}^{t+\Delta t} \underline{\underline{\mathbf{F}}}_p = \hat{\underline{\underline{\mathbf{F}}}}_p$$

$${}^{t+\Delta t} \underline{\underline{\mathbf{T}}}_D = \hat{\underline{\underline{\mathbf{T}}}}_D$$

ELSE

go to plastic corrector

*Plastic corrector*

$$\Delta \bar{\epsilon}_p = \frac{\hat{\phi}}{(3G + h)}$$

$G$  : shear modulus of the elastic law

$h$  : hardening modulus

$${}^{t+\Delta t} \underline{\underline{\mathbf{T}}}}_D = \hat{\underline{\underline{\mathbf{T}}}}_D - \sqrt{6} G \Delta \bar{\epsilon}_p \frac{\hat{\underline{\underline{\mathbf{T}}}}_D}{\sqrt{\hat{\underline{\underline{\mathbf{T}}}}_D : \hat{\underline{\underline{\mathbf{T}}}}_D}}$$

The above equation clearly displays the *radial return property* of the plastic corrector algorithm.

We obtain  ${}^{t+\Delta t} \underline{\underline{\mathbf{T}}}_D$  remembering that in the case of associated Von Mises flow rule the hydrostatic stress is only related to the elastic deformations.

Also,

$${}^t \underline{\underline{\mathbf{F}}}_p = \exp \left( \sqrt{\frac{3}{2}} \Delta \bar{\epsilon}_p \frac{\hat{\underline{\underline{\mathbf{T}}}}_D}{\sqrt{\hat{\underline{\underline{\mathbf{T}}}}_D : \hat{\underline{\underline{\mathbf{T}}}}_D}} \right) \cdot {}^t \underline{\underline{\mathbf{F}}}_p$$

$${}^{t+\Delta t} \sigma_y = {}^t \sigma_y + \beta h \Delta \bar{\epsilon}_p$$

**Box II**

Using the Kirchhoff stress tensor we can integrate on the reference volume ( ${}^\circ V$ ), hence

$$\int_{{}^\circ V} {}^{t+\Delta t} \tau^{ij} \delta e_{ij} {}^\circ dV = {}^{t+\Delta t} \mathfrak{R} \quad (73.b)$$

For an elastically isotropic material [46]

$${}^{t+\Delta t} \tau^{ij} \delta e_{ij} = {}^{t+\Delta t} \Gamma^{IJ} \delta (H_e)_{IJ} \quad (74)$$

where  ${}^{t+\Delta t} \Gamma^{IJ}$  is defined by Eqn. (55).

Therefore we can rewrite Eqn. (73.b) as

$$\int_{{}^\circ V} {}^{t+\Delta t} \Gamma^{IJ} \delta (H_e)_{IJ} {}^\circ dV = {}^{t+\Delta t} \mathfrak{R} \quad (75)$$

Since we are interpolating total Hencky strain components rather than elastic Hencky strain components, we have to use in Eqn. (75)

$$\delta (H_e)_{IJ} = \frac{\partial (H_e)_{IJ}}{\partial H_{KL}} \delta H_{KL} \quad (76)$$

The fourth order tensor  $\left( \frac{\partial (H_e)_{IJ}}{\partial H_{KL}} \right)$  is calculated at every Gauss point (see Appendix I). Note that it cannot be calculated at the sampling points because *the tensor  ${}^\circ \underline{\underline{\mathbf{F}}}_p$  is only known at the Gauss points.*

We can now rewrite Eqn. (75) as

$$\int_{{}^\circ V} {}^{t+\Delta t} \Gamma^{IJ} \frac{\partial (H_e)_{IJ}}{\partial H_{KL}} \delta H_{KL} {}^\circ dV = {}^{t+\Delta t} \mathfrak{R} \quad (77)$$

### 5.5.1 Linearization of the equilibrium equations

The nonlinear equilibrium equations (77) are solved using a Newton-Raphson iterative scheme, with the possible addition of a line search algorithm [57].

For the  $(i+1)$ -th iteration, the linearized equation is

$$\begin{aligned} & \int_{{}^\circ V} d\Gamma^{IJ} \left( \frac{\partial (H_e)_{IJ}}{\partial H_{KL}} \right)^{(i)} \delta H_{KL} {}^\circ dV + \int_{{}^\circ V} [{}^{t+\Delta t} \Gamma^{(i)}]^{IJ} d \left[ \frac{\partial (H_e)_{IJ}}{\partial H_{KL}} \delta H_{KL} \right] {}^\circ dV = \\ & {}^{t+\Delta t} \mathfrak{R} - \int_{{}^\circ V} [{}^{t+\Delta t} \Gamma^{(i)}]^{IJ} \left[ \frac{\partial (H_e)_{IJ}}{\partial H_{KL}} \right]^{(i)} \delta H_{KL} {}^\circ dV \end{aligned} \quad (78)$$

When linearizing we use the following relations

$${}^{t+\Delta t} \underline{\underline{\mathbf{\Gamma}}} = {}^{t+\Delta t} \underline{\underline{\mathbf{\Gamma}}} [{}^{t+\Delta t} \underline{\underline{\mathbf{u}}}; {}^{t+\Delta t} \underline{\underline{\xi}}; {}^{t+\Delta t} \underline{\underline{\mathbf{e}}}_p] \quad (79.a)$$

$${}^\circ \underline{\underline{\mathbf{H}}}_e = {}^\circ \underline{\underline{\mathbf{H}}}_e [{}^{t+\Delta t} \underline{\underline{\mathbf{u}}}; {}^{t+\Delta t} \underline{\underline{\xi}}; {}^{t+\Delta t} \underline{\underline{\mathbf{e}}}_p] \quad (79.b)$$

The derivatives in Eqn. (78) are developed in Appendix I.

Also we use

$$\delta H_{KL} = 2 \left. \frac{\partial H_{KL}}{\partial C_{PQ}} \right|^{(i)} \delta \varepsilon_{PQ} \quad (80)$$

where  $\delta\varepsilon_{PQ}$  is the variation of the Green-Lagrange strain tensor covariant components. The expression for this variation in terms of the displacements variation is given in Ref. [6].

For the derivation of the fourth order tensor  $\left(\frac{\partial H_{\kappa\lambda}}{\partial C_{PQ}}\right)^{(i)}$  see Appendix I.

For calculating  $d\underline{\underline{\underline{\Gamma}}}$  we use

- In the case of *elastic loading / unloading*

$$d\underline{\underline{\underline{\Gamma}}} = \underline{\underline{\underline{\mathbf{C}}}} : d\underline{\underline{\underline{\hat{\mathbf{H}}}}}_e \quad (81.a)$$

- In the case of *plastic loading* we have to determine a  $d\underline{\underline{\underline{\Gamma}}}$  consistent with the radial return algorithm.

From the equations developed for the plastic corrector phase we get,

$${}^{t+\Delta t}\underline{\underline{\underline{\Gamma}}}_D = 2 G \left[ \underline{\underline{\underline{\hat{\mathbf{H}}}}}_{eD} - {}^{t+\Delta t}\lambda \ {}^{t+\Delta t}\underline{\underline{\underline{\Gamma}}}_D \right] \quad (81.b)$$

where  ${}^{t+\Delta t}\lambda = \frac{3}{2} \frac{\Delta\bar{\varepsilon}_p}{{}^{t+\Delta t}\sigma_y}$ .

Differentiating Eqn. (81.b) we get

$$d\underline{\underline{\underline{\Gamma}}}_D = 2 G \left[ d\underline{\underline{\underline{\hat{\mathbf{H}}}}}_{eD} - d\lambda \ {}^t\underline{\underline{\underline{\Gamma}}}_D - {}^t\lambda \ d\underline{\underline{\underline{\Gamma}}}_D \right] \quad (81.c)$$

Therefore

$$d\underline{\underline{\underline{\Gamma}}}_D = \frac{2 G}{1 + 2 G \ {}^t\lambda} \left[ d\underline{\underline{\underline{\hat{\mathbf{H}}}}}_{eD} - d\lambda \ {}^t\underline{\underline{\underline{\Gamma}}}_D \right] \quad (81.d)$$

From the *consistency condition*  ${}^t\dot{\phi} = 0$  and using the evolution equation (59) together with the above we get

$$d\lambda = \frac{9 G \left(1 - \frac{2}{3} h \ {}^t\lambda\right)}{2 \ {}^t\sigma_y^2 \ (3 G + h)} \ {}^t\underline{\underline{\underline{\Gamma}}}_D : d\underline{\underline{\underline{\hat{\mathbf{H}}}}}_{eD} \quad (81.e)$$

Hence, replacing in Eqn. (81.d)

$$d\underline{\underline{\underline{\Gamma}}}_D = \frac{2 G}{1 + 2 G \ {}^t\lambda} \left[ \underline{\underline{\underline{\mathbf{I}}}} - {}^t\chi_3 \ {}^t\underline{\underline{\underline{\Gamma}}}_D \ {}^t\underline{\underline{\underline{\Gamma}}}_D \right] : d\underline{\underline{\underline{\hat{\mathbf{H}}}}}_{eD} \quad (81.f)$$

in the above  $\underline{\underline{\underline{\mathbf{I}}}}$  is the fourth order unit tensor and

$${}^t\chi_3 = \frac{9 G \left(1 - \frac{2}{3} h \ {}^t\lambda\right)}{2 \ {}^t\sigma_y^2 \ (3 G + h)} \quad (81.g)$$

We can rewrite Eqn. (81.f) as

$$d\underline{\underline{\underline{\Gamma}}}_D = \frac{2 G}{1 + 2 G \ {}^t\lambda} \left[ \underline{\underline{\underline{\mathbf{I}}}}_{DEV} - {}^t\chi_3 \ {}^t\underline{\underline{\underline{\Gamma}}}_D \ {}^t\underline{\underline{\underline{\Gamma}}}_D \right] : d\underline{\underline{\underline{\hat{\mathbf{H}}}}}_e \quad (81.h)$$

In the above [25]

$$\underline{\underline{\underline{\mathbf{I}}}}_{DEV} = \underline{\underline{\underline{\mathbf{I}}}} - \frac{1}{3} \underline{\underline{\underline{\mathbf{g}}}} \underline{\underline{\underline{\mathbf{g}}}} \quad (81.i)$$

where  $\underline{\underline{\underline{\mathbf{g}}}} = {}^tR_e^* \left( {}^t\underline{\underline{\underline{\mathbf{g}}}} \right)$  and  ${}^t\underline{\underline{\underline{\mathbf{g}}}}$  is the metric tensor of the spatial configuration.

For a material behavior described by the associated von Mises flow rule and a linear isotropic elastic relation

$$d\underline{\underline{\Gamma}} = \left\{ \frac{2 G}{1 + 2 G t\lambda} \left[ \underline{\underline{\mathbf{I}}}_{DEV} - t\chi_3 t\underline{\underline{\Gamma}}_D t\underline{\underline{\Gamma}}_D \right] + \frac{E}{3(1 - 2\nu)} \underline{\underline{\mathbf{g}}} \underline{\underline{\mathbf{g}}} \right\} : d\underline{\underline{\hat{\Gamma}}}_e \quad (81.j)$$

The fourth order tensor between brackets on the r.h.s. of the above equation is the *algorithmic consistent tangent constitutive tensor* [59-61] ( $t\underline{\underline{\mathbf{C}}}_{EP}$ ).

It is important to realize that

$$({}_tC_{EP})^{IJKL} = ({}_tC_{EP})^{JIKL} = ({}_tC_{EP})^{IJLK} = ({}_tC_{EP})^{KLIJ} \quad (82)$$

In order to illustrate on the behavior of the MITC4-TLH shell element in finite strain elasto-plastic analysis we present two examples in Figures 23 and 24.

### CONCLUSIONS

The formulation of general shell elements using the method of *mixed interpolation of tensorial components* was reviewed.

For problems in which the hypothesis of small strain deformations is valid, the formulation and performance of the MITC4 and MITC8 shell elements was analyzed in detail.

The formulation of the MITC4-TLH shell element for finite strain elasto-plastic problems was also analyzed.

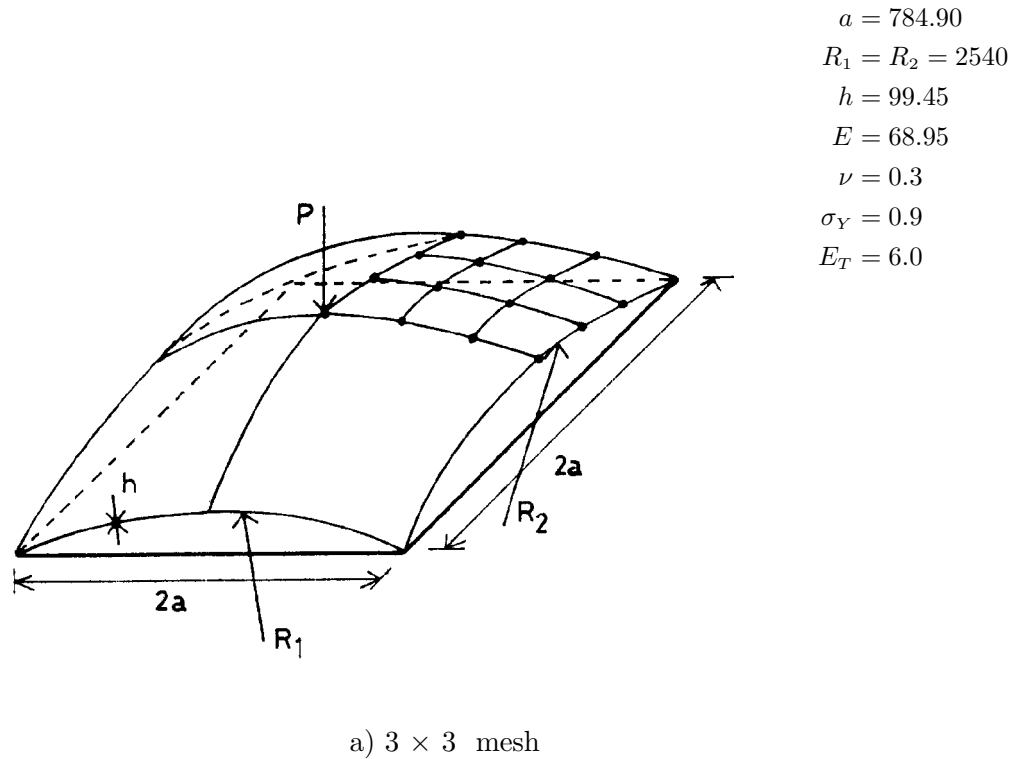
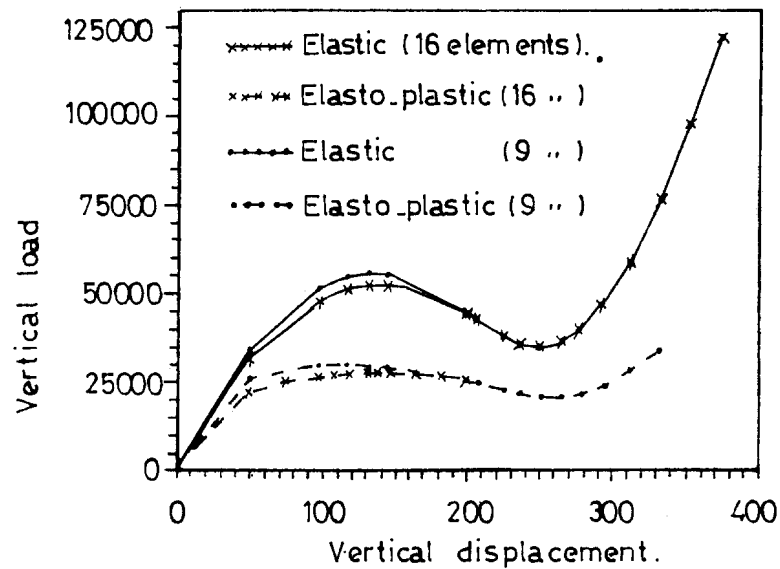
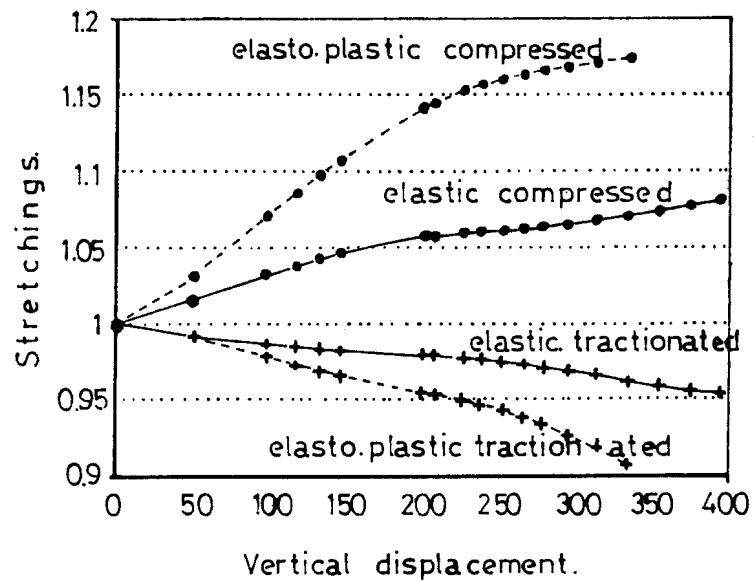


**Figure 23.** Finite strain elasto-plastic analysis of a spherical shell (MITC4-TLH)

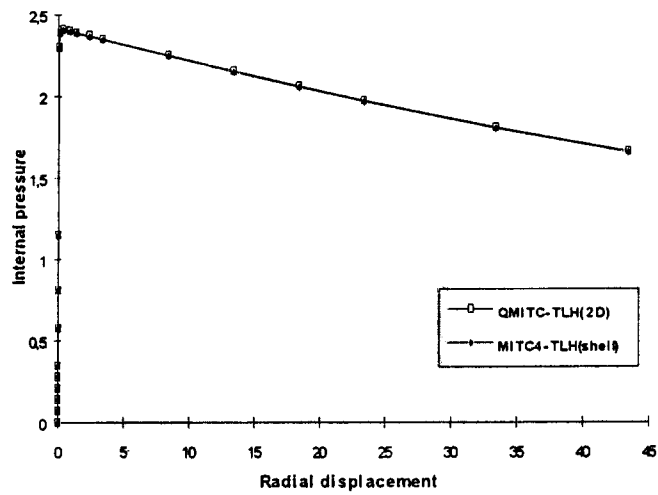
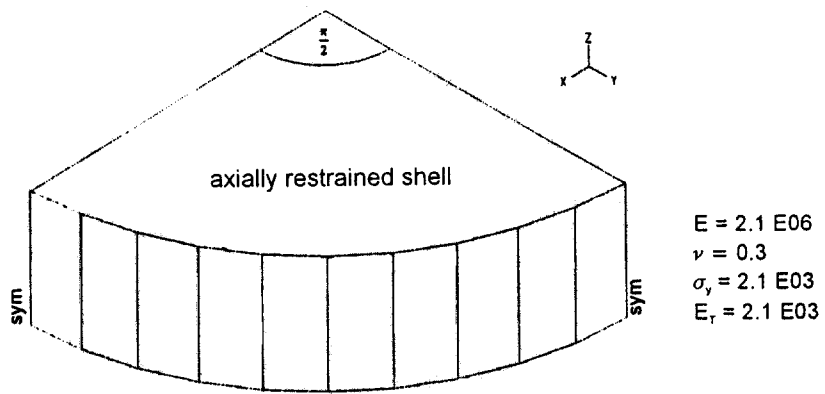


b) Vertical load vs. vertical displacement.

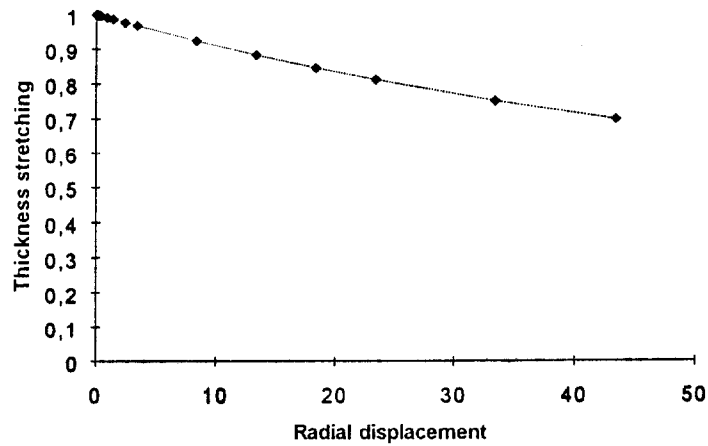


c) Through the thickness stretchings at the Gauss points closest to the center (top and bottom).

Figure 23. (Continued)



(a) Pressure vs. displacement



(b) Thickness stretching at external layer of Gauss points

Figure 24. Inflation of an elasto-plastic cylinder

## REFERENCES

- 1 Ahmad, S., Irons, B.M. and Zienkiewicz, O.C. (1970), "Analysis of thick and thin shell structures by curved finite elements", *Int. J. Num. Meth. Engrg.*, **2**, pp. 419–451.
- 2 Zienkiewicz, O.C. and Taylor, R.L. (1989), "*The Finite Element Method*", (Fourth Edition), Mc Graw Hill.
- 3 Reissner, E. (1945), "The effect of transverse shear deformation on the bending of elastic plates", *J. Appl. Mech.*, **12**, pp. 69–76.
- 4 Mindlin, R.D. (1951), "Influence of rotatory inertia and shear in flexural motions of isotropic elastic plates", *J. Appl. Mech.*, **18**, pp. 31–38.
- 5 Bathe, K.J. and Bolourchi, S. (1979), "A geometric and material nonlinear plate and shell element", *Comput. & Struct.*, **11**, pp. 23–48.
- 6 Bathe, K.J. (1982), "*Finite Element Procedures in Engineering Analysis*", Prentice-Hall, Englewood Cliffs, New Jersey.
- 7 Ramm, E. (1977), "A plate / shell element for large deflections and rotations" in *Formulations and Computational Algorithms in Finite Element Analysis*, (Eds. K.J. Bathe et. al.), M.I.T. Press.
- 8 Kråkeland, B. (1978), "Nonlinear analysis of shells using degenerate isoparametric elements", in *Finite Elements in Nonlinear Mechanics*, Tapir Publishers.
- 9 Dvorkin, E.N. (1984), *On Nonlinear Finite Element Analysis of Shell Structures*, Ph.D. Thesis, Dept. of Mech. Eng., M.I.T., Cambridge, Mass., U.S.A.
- 10 Dvorkin, E.N. and Bathe, K.J. (1984), "A continuum mechanics based four node shell element for general nonlinear analysis", *Engrg. Comput.*, **1**, pp. 77–88.
- 11 Bathe, K.J. and Dvorkin, E.N. (1985), "A four-node plate bending element based on Mindlin/Reissner plate theory and a mixed interpolation", *Int. J. Num. Meth. Engrg.*, **21**, pp. 367–383.
- 12 Bathe, K.J. and Dvorkin, E.N. (1986), "A formulation of general shell elements – the use of mixed interpolation of tensorial components", *Int. J. Num. Meth. Engrg.*, **22**, pp. 697–722.
- 13 Dvorkin, E.N. (1992), "On nonlinear analysis of shells using finite elements based on mixed interpolation of tensorial components", in *Nonlinear Analysis of Shells by Finite Elements*, (Ed. F.G. Rammerstorfer), Springer Verlag.
- 14 Bathe, K.J., Dvorkin, E.N. and Ho, L.W. (1983), "Our discrete Kircchoff and isoparametric shell elements for nonlinear analysis -an assessment", *Comput. & Struct.*, **16**, pp. 89–98.
- 15 Belytschko, T, Stolarski, H., Liu, W.K., Carpenter, N. and Ong, J. (1985), "Stress projection for membrane and shear locking in shell finite elements", *Comput. Methods Appl. Mech. Engrg.*, **51**, pp. 221–258.
- 16 Zienkiewicz, O.C., Taylor R.L. and Too, J.M. (1971), "Reduced integration techniques in general analysis of plates and shells", *Int. J. Num. Meth. Engrg.*, **3**, pp. 275–290.
- 17 Hughes, T.J.R. (1987), "*The Finite Element Method*", Prentice-Hall, Englewood Cliffs, NJ.
- 18 Malkus, D.S. and Hughes, T.J.R. (1978), "Mixed finite element methods in reduced and selective integration techniques: a unification of concepts", *Comput. Methods Appl. Mech. Engrg.*, **15**, pp. 63–81.

- 19 Crisfield, M.A. (1986), “*Finite Elements and Solution Procedures for Structural Analysis. Vol.I: Linear Analysis*”, Pineridge Press, Swansea.
- 20 Belytschko, T. and Tsay, C.S. (1983), “A stabilization procedure for the quadrilateral plate element with one-point quadrature”, *Int. J. Num. Meth. Engrg.*, **19**, pp. 405–419.
- 21 Belytschko, T. and Leviathan, I. (1994), “Projection schemes for one-point quadrature shell elements”, *Comput. Methods Appl. Mech. Engrg.*, **115**, pp. 277–286.
- 22 Irons, B.M. and Razzaque, A. (1972), “Experience with the patch test for convergence of finite elements”, in *The Mathematical Foundations of the Finite Element Method with Applications to Partial Differential Equations*, (Ed. A.K. Aziz), Academic Press.
- 23 Dvorkin, E.N., Pantuso, D. and Repetto, E. A., “A formulation of the MITC4 shell element for finite strain elasto-plastic analysis”, *Comput. Methods Appl. Mech. Engrg.*(in press).
- 24 Strang, G. and Fix, G.J. (1973.), “*An Analysis of the Finite Element Method*”, Prentice Hall.
- 25 Marsden, J.E. and Hughes, T.J.R. (1983), “*Mathematical Foundations of Elasticity*”, Prentice-Hall, Englewood Cliffs, New Jersey.
- 26 Dvorkin, E.N., Goldschmit, M.B., Pantuso, D. and Repetto, E.A. (1994), “Comentarios sobre algunas herramientas utilizadas en la resolución de problemas no-lineales de mecánica del continuo”, *Rev. Int. de Met. Numéricos para Cálculo y Diseño en Ingeniería*, **10**, pp. 47–65.
- 27 Truesdell, C. and Noll, W. (1965), “The nonlinear field theories of mechanics”, in *Encyclopedia of Physics*, Springer, Berlin.
- 28 Malvern, L.E. (1969), “*Introduction to the Mechanics of a Continuous Medium*”, Prentice-Hall, Englewood Cliffs, New Jersey.
- 29 Simo, J.C. and Taylor, R.L. (1985), “Consistent tangent operators for rate-independent plasticity”, *Comput. Methods Appl. Mech. Engrg.*, **48**, pp. 101–118.
- 30 Simo, J.C. and Taylor, R.L. (1986), “A return mapping algorithm for plane stress elasto-plasticity”, *Int. J. Num. Meth. Engrg.*, **22**, pp. 649–670.
- 31 Ortiz, M. and Simo, J.C. (1986), “An analysis of a new class of integration algorithms for elastoplastic constitutive relations”, *Int. J. Num. Meth. Engrg.*, **23**, pp. 353–366.
- 32 Bathe, K.J. and Cimento, A.P. (1980), “Some practical procedures for the solution of nonlinear finite element equations”, *Comput. Methods Appl. Mech. Engrg.*, **22**, pp. 59–85.
- 33 Bathe, K.J. and Dvorkin, E.N. (1983), “On the automatic solution of nonlinear finite element equations”, *Comput. & Struct.*, **17**, pp. 871–879.
- 34 Dvorkin, E.N., Oñate, E. and Oliver, J. (1988), “On a non-linear formulation for curved Timoshenko beam elements considering large displacement/rotation increments”, *Int. J. Num. Meth. Engrg.*, **26**, pp. 1597–1613.
- 35 Argyris, J. (1982), “An excursion into large rotations”, *Comput. Methods Appl. Mech. Engrg.*, **32**, pp. 85–155.
- 36 Lee, E.H. and Liu, D.T. (1967), “Finite strain elastic-plastic theory with application to plane-wave analysis”, *J. Appl. Phys.*, **38**, pp. 17–27.
- 37 Lee, E.H. (1969), “Elastic plastic deformation at finite strain”, *J. Appl. Mech.*, **36**, pp. 1–6.
- 38 Argyris, J.H. and Doltsinis, J. St. (1979), “On the large strain inelastic analysis in natural formulation. Part I. Quasistatic problems.”, *Comput. Methods Appl. Mech. Engrg.*, **20**, pp. 213–251.

- 39 Argyris, J.H. and Doltsinis, J. St. (1980), "On the large strain inelastic analysis in natural formulation. Part II. Dynamic problems.", *Comput. Methods Appl. Mech. Engrg.*, **21**, pp. 91–126.
- 40 Simo, J.C. and Ortiz, M. (1985), "A unified approach to finite deformation elastoplasticity based on the use of hyperelastic constitutive equations", *Comput. Methods Appl. Mech. Engrg.*, **51**, pp. 177–208.
- 41 Simo, J.C. (1988), "A. Framework for finite strain elasto-plasticity based on maximum plastic dissipation and the multiplicative decomposition, part I: Continuum formulation", *Comput. Methods Appl. Mech. Engrg.*, **66**, pp. 199–219.
- 42 Simo, J.C. (1988), "A. Framework for finite strain elasto-plasticity based on maximum plastic dissipation and the multiplicative decomposition, part II: Computational aspects", *Comput. Methods Appl. Mech. Engrg.*, **68**, pp. 1–31.
- 43 Hill, R. (1950), "*The Mathematical Theory of Plasticity*", Oxford University Press.
- 44 Dvorkin, E.N., Pantuso, D. and Repetto, E.A. (1994), "A finite element formulation for finite strain elasto-plastic analysis based on mixed interpolation of tensorial components", *Comput. Methods Appl. Mech. Engrg.*, **114**, pp. 35–54.
- 45 Hill, R. (1978), "Aspects of invariance in solid mechanics", *Advances in Appl. Mech.*, **18**, pp. 1–75.
- 46 Atluri, S.N. (1984), "Alternate stress and conjugate strain measures, and mixed variational formulations involving rigid rotations for computational analysis of finitely deformed solids, with applications to plates and shells. Part I", *Comput. & Struct.*, **18**, pp. 93–116.
- 47 Krauss, H. (1967), "*Thin Elastic Shells*", John Wiley & Sons, New York.
- 48 Rodal, J.J.A. and Witmer, E.A. (1979), "Finite-strain large-deflection elastic-viscoplastic finite-element transient analysis of structures", NASA CR 159874.
- 49 Hughes, T.J.R. and Carnoy, E. (1983), "Nonlinear finite element shell formulation accounting for large membrane strains", *Comput. Methods Appl. Mech. Engrg.*, **39**, pp. 69–82.
- 50 Simo, J.C. and Fox, D.D. (1989), "On a stress resultant geometrically exact shell model. Part I: Formulation and optimal parametrization", *Comput. Methods Appl. Mech. Engrg.*, **72**, pp. 267–304.
- 51 Simo, J.C. Fox, D.D. and Rifai, M.S. (1989), "On a stress resultant geometrically exact shell model. Part II: The linear theory; Computational aspects", *Comput. Methods Appl. Mech. Engrg.*, **73**, pp. 53–92.
- 52 Simo, J.C. Fox, D.D. and Rifai, M.S. (1990), "On a stress resultant geometrically exact shell model. Part III: Computational aspects of the nonlinear theory", *Comput. Methods Appl. Mech. Engrg.*, **79**, pp. 21–70.
- 53 Simo, J.C. Fox, D.D. and Rifai, M.S. (1990), "On a stress resultant geometrically exact shell model. Part IV: Variable thickness shells with through-the-thickness stretching", *Comput. Methods Appl. Mech. Engrg.*, **81**, pp. 91–126.
- 54 Simo, J.C. and Kennedy, J.G. (1992), "On a stress resultant geometrically exact shell model. Part V: Nonlinear plasticity formulation and integration algorithms", *Comput. Methods Appl. Mech. Engrg.*, **96**, pp. 133–171.
- 55 Simo, J.C., Marsden, J. E. (1984), "On the rotated stress tensor and the material version of the Doyle Ericksen formula", *Arch. Rat. Mech. Anal.*, **86**, pp. 213–231.

- 56 Lubliner, J. (1990), “*Plasticity Theory*”, Macmillan.
- 57 Luenberger, D.G. (1984), “*Linear and Nonlinear Programming*”, Addison-Wesley, Reading, MA.
- 58 Eterovic, A.L. and Bathe, K.J. (1990), “A hyperelastic based large strain elasto-plastic constitutive formulation with combined isotropic/kinematic hardening using the logarithmic stress and strain measures”, *Int. J. Num. Meth. Engrg.*, **30**, pp. 1099–1114.
- 59 Ortiz, M. and Simo, J.C. (1986), “An analysis of a new class of integration algorithms for elastoplastic constitutive relations”, *Int. J. Num. Meth. Engrg.*, **23**, pp. 353–366.
- 60 Simo, J.C. and Taylor, R. L. (1985), “Consistent tangent operators for rate-independent plasticity”, *Comput. Methods Appl. Mech. Engrg.*, **48**, pp. 101–118.
- 61 Simo, J.C. and Taylor, R.L. (1986), “A return mapping algorithm for plane stress elasto-plasticity”, *Int. J. Num. Meth. Engrg.*, **22**, pp. 649–670.

## APPENDIX I

### I.1 Derivates of ${}^t\tau^{nn}$

We can write

$${}^t\tau^{nn} = {}^t\mathbf{V}_n \cdot [ {}^t\underline{\mathbf{R}}_e \cdot {}^t\underline{\mathbf{\Gamma}} \cdot {}^t\underline{\mathbf{R}}_e^T ] \cdot {}^t\mathbf{V}_n \quad (\text{I.1})$$

then

$$\frac{\partial {}^t\tau^{nn}}{\partial {}^t\xi_q} = {}^t\mathbf{V}_n \cdot \left[ 2 \text{sym} \left( \frac{\partial {}^t\underline{\mathbf{R}}_e}{\partial {}^t\xi_q} \cdot {}^t\underline{\mathbf{\Gamma}} \cdot {}^t\underline{\mathbf{R}}_e^T \right) + {}^t\underline{\mathbf{R}}_e \cdot \frac{\partial {}^t\underline{\mathbf{\Gamma}}}{\partial {}^t\xi_q} \cdot {}^t\underline{\mathbf{R}}_e^T \right] \cdot {}^t\mathbf{V}_n \quad (\text{I.2})$$

Since  ${}^t\underline{\mathbf{F}}^{DI} = {}^t\underline{\mathbf{F}}^{DI}({}^t\underline{\mathbf{u}}, {}^t\xi)$ , it is immediate to calculate the derivatives of  ${}^t\underline{\mathbf{F}}^{DI}$ ,  ${}^t\underline{\mathbf{U}}^{DI}$ ,  ${}^t\underline{\mathbf{R}}^{DI}$  and  ${}^t\underline{\mathbf{H}}^{DI}$  with respect to  ${}^t\xi_q$ , and therefore of the interpolated values  ${}^t\underline{\mathbf{H}}$ . Using Eqns. (47) we can calculate the derivatives of  ${}^t\underline{\mathbf{F}}$ ,  ${}^t\underline{\mathbf{U}}$  and  ${}^t\underline{\mathbf{R}}$ .

We can write

$${}^t\underline{\mathbf{R}}_e = {}^t\underline{\mathbf{F}}^{DI} \cdot ({}^t\underline{\mathbf{U}}^{DI})^{-1} \cdot {}^t\underline{\mathbf{U}} \cdot {}^t\underline{\mathbf{F}}_p^{-1} \cdot {}^t\underline{\mathbf{U}}_e^{-1} \quad (\text{I.3})$$

and considering that

$$\left. \frac{\partial {}^t\underline{\mathbf{F}}_p}{\partial {}^t\xi_q} \right|_{\bar{\epsilon}_p} = \underline{\mathbf{0}} \quad (\text{I.4.a})$$

$$\frac{\partial {}^t\underline{\mathbf{U}}_e}{\partial {}^t\xi_q} = \frac{\partial {}^t\underline{\mathbf{U}}_e}{\partial {}^t\underline{\mathbf{C}}_e} : \frac{\partial {}^t\underline{\mathbf{C}}_e}{\partial {}^t\underline{\mathbf{C}}} : \frac{\partial {}^t\underline{\mathbf{C}}}{\partial {}^t\underline{\mathbf{H}}} : \frac{\partial {}^t\underline{\mathbf{H}}}{\partial {}^t\xi_q} \quad (\text{I.4.b})$$

we can calculate  $\frac{\partial {}^t\underline{\mathbf{R}}_e}{(\partial {}^t\xi_q)}$  using the fourth order tensor we will develop in Section I.3 and replace in Eqn. (I.2).

Also in Eqn. (I.2) we use

$$\frac{\partial {}^t\underline{\mathbf{\Gamma}}}{\partial {}^t\xi_q} = \frac{\partial {}^t\underline{\mathbf{\Gamma}}}{\partial {}^t\underline{\mathbf{H}}_e} : \frac{\partial {}^t\underline{\mathbf{H}}_e}{\partial {}^t\underline{\mathbf{C}}_e} : \frac{\partial {}^t\underline{\mathbf{C}}_e}{\partial {}^t\underline{\mathbf{C}}} : \frac{\partial {}^t\underline{\mathbf{C}}}{\partial {}^t\underline{\mathbf{H}}} : \frac{\partial {}^t\underline{\mathbf{H}}}{\partial {}^t\xi_q} \quad (\text{I.5})$$

again, to calculate the above expression we have to resort to the fourth order tensor we will develop in Section I.3.

## I.2 Derivatives used in the linearization of the equilibrium equations

- At each sampling point we have  ${}^t\underline{\underline{\underline{\mathbf{H}}}}^{DI}$ ,  $d\underline{\underline{\underline{\mathbf{H}}}}^{DI}$  and  $d(\delta\underline{\underline{\underline{\mathbf{H}}}}^{DI})$  that can be interpolated to obtain  ${}^t\underline{\underline{\mathbf{H}}}$ ,  $d\underline{\underline{\mathbf{H}}}$  and  $d(\delta\underline{\underline{\mathbf{H}}})$  at the Gauss points. When calculating the derivatives it is important to take into account that [34]

$$d\underline{\underline{\mathbf{V}}}_n = d\theta_2 \quad {}^t\underline{\underline{\mathbf{V}}}_1 - d\theta_1 \quad {}^t\underline{\underline{\mathbf{V}}}_2 \quad (\text{I.6.a})$$

$$d(\delta\underline{\underline{\mathbf{V}}}_n) = -(\delta\theta_1 \, d\theta_1 + \delta\theta_2 \, d\theta_2) \quad {}^t\underline{\underline{\mathbf{V}}}_n \quad (\text{I.6.b})$$

- To calculate  ${}^t\underline{\underline{\underline{\mathbf{H}}}}_e$ ,  $d \quad {}^t\underline{\underline{\underline{\mathbf{H}}}}_e$  and  $d(\delta \quad {}^t\underline{\underline{\underline{\mathbf{H}}}}_e)$  at the Gauss points we use the accumulated value of  ${}^t\underline{\underline{\underline{\mathbf{F}}}}_p$  at those points ante the fourth order tensor we will develop in I.3 also calculated at the Gauss points.
- Starting from the condition  ${}^t\tau^{nn} = 0$  we can calculate

$$\frac{\partial \quad {}^t\xi_q}{\partial \quad {}^t u_A} = - \left[ \frac{\partial \quad {}^t\tau^{nn}}{\partial \quad {}^t\xi_q} \right]^{-1} \frac{\partial \quad {}^t\tau^{nn}}{\partial \quad {}^t u_A} \quad (\text{I.7})$$

- In our Ref. [44] we defined for 2D problems the fourth order tensor.

## I.3 $\partial \quad {}^t\underline{\underline{\underline{\mathbf{H}}}}_e / \partial \quad {}^t\underline{\underline{\mathbf{H}}}$

In our Ref. [44] we defined for 2D problems the fourth order tensor

$${}^t\underline{\underline{\underline{\underline{\mathbf{D}}}}} = \frac{\partial \quad {}^t\underline{\underline{\underline{\mathbf{H}}}}_e}{\partial \quad {}^t\underline{\underline{\mathbf{H}}}} \quad (\text{I.8})$$

We calculate

$${}^t\underline{\underline{\underline{\underline{\mathbf{D}}}}} = \frac{\partial \quad {}^t\underline{\underline{\underline{\mathbf{H}}}}_e}{\partial \quad {}^t\underline{\underline{\underline{\mathbf{C}}}}_e} : \frac{\partial \quad {}^t\underline{\underline{\underline{\mathbf{C}}}}_e}{\partial \quad {}^t\underline{\underline{\underline{\mathbf{C}}}}_e} : \frac{\partial \quad {}^t\underline{\underline{\underline{\mathbf{C}}}}_e}{\partial \quad {}^t\underline{\underline{\mathbf{H}}}} \quad (\text{I.9})$$

To calculate the first term on the r.h.s. of Eqn.(I.9) we construct  ${}^t\underline{\underline{\underline{\mathbf{H}}}}_e$  using the eigenvectors and eigenvalues of  ${}^t\underline{\underline{\underline{\mathbf{C}}}}_e$ .

To calculate the second term on the r.h.s. of Eqn.(I.9) we use

$${}^t\underline{\underline{\underline{\mathbf{C}}}}_e = {}^t\underline{\underline{\underline{\mathbf{F}}}}_p^{-T} \cdot {}^t\underline{\underline{\underline{\mathbf{C}}}} \cdot {}^t\underline{\underline{\underline{\mathbf{F}}}}_p^{-1} \quad (\text{I.10})$$

To calculate the third term on the r.h.s. of Eqn. (I.9) we construct  ${}^t\underline{\underline{\underline{\mathbf{C}}}}_e$  using the eigenvalues and eigenvectors of  ${}^t\underline{\underline{\underline{\mathbf{H}}}}_e$ .

For the cases where we arrive to multiple eigenvalues we introduce small perturbations [44].

Please address your comments or questions on this paper to:  
 International Center for Numerical Methods in Engineering  
 Edificio C-1, Campus Norte UPC  
 Gran Capitán s/n  
 08034 Barcelona, Spain  
 Phone: 34-93-4016035; Fax: 34-93-4016517  
 E-mail: onate@cimne.upc.es